JOURNAL OF GEOPHYSICAL RESEARCH, VOL. 103, NO. D11, PAGES 13,451–13,476, JUNE 20, 1998

Export of reactive nitrogen from North America during summertime: Sensitivity to hydrocarbon chemistry

Larry W. Horowitz,[1] Jinyou Liang,[2] Geraldine M. Gardner, and Daniel J. Jacob

Division of Engineering and Applied Sciences and Department of Earth and Planetary Sciences, Harvard University, Cambridge, Massachusetts

Abstract. The global influence on tropospheric chemistry of nitrogen oxides (NO_x=NO+NO_2) emitted by fossil fuel combustion may be strongly modulated by nonmethane hydrocarbon (NMHC) chemistry taking place in the continental boundary layer. This effect is investigated using a three-dimensional, continental-scale model of tropospheric O_3-NO_x-NMHC chemistry over North America in summer. The model includes detailed representation of NMHC chemistry including in particular isoprene. Model results are evaluated with observations for ozone, reactive nitrogen species, and photochemical tracers at a number of sites in North America. Sensitivity analyses are conducted to explore the effects of assumptions regarding the aerosol chemistry of peroxy radicals and the fate of hydroxy organic nitrates produced from the oxidation of isoprene. A budget analysis for the United States in the model indicates that 9% of NO_x emitted from fossil fuel combustion is exported out of the continental boundary layer as NO_x, 3.5% is exported as peroxyacetyl nitrate (PAN), and 3.7% is exported as other organic nitrates. Isoprene is the principal NMHC responsible for the formation and export of organic nitrates, which eventually decompose to provide a source of NO_x in the remote troposphere. Export of NO_x and organic nitrates from the U.S. boundary layer is found to be a major source of NO_x on the scale of the northern hemisphere troposphere and on the scale of the upper troposphere at northern midlatitudes. Proper representation of isoprene chemistry in the continental boundary layer is important for simulation of NO_x in global tropospheric chemistry models.

1. Introduction

Ozone is produced in the troposphere by photochemical oxidation of hydrocarbons and CO in the presence of nitrogen oxides (NO_x = NO+NO_2). In industrial regions with large anthropogenic sources of NO_x and hydrocarbons, high concentrations of surface ozone represent a threat to public health and vegetation [*National Research Council*, 1991]. On a global scale, tropospheric ozone plays a critical role in controlling the oxidizing power of the atmosphere [*Thompson*, 1992] and is an important greenhouse gas [*Hansen et al.*, 1997]. Several studies have suggested that export of anthropogenic NO_x from industrial continents could make a large global contribution to ozone [*Liu et al.*, 1987; *Jacob et al.*, 1993a; *Mauzerall et al.*, 1996], thus linking regional air pollution and global tropospheric chemistry issues. Accounting for this anthropogenic source of ozone in global models requires an estimate of the export of NO_x out of the continental boundary layer; complications arise because of the short lifetime of NO_x against oxidation to HNO_3 (less than a day) and because of the presence in the continental boundary layer of high concentrations of reactive nonmethane hydrocarbons (NMHCs). These NMHCs modify the chemistry of the continental boundary layer in several ways, including the formation of organic nitrates such as peroxyacetyl nitrate (PAN). The organic nitrates can be exported out of the continental boundary layer and provide reservoirs of NO_x in the global troposphere [*Crutzen*, 1979], thus contributing to the anthropogenic influence on ozone.

The object of this paper is to improve understanding of the export of NO_x and its reservoirs out of the continental boundary layer over the United States in summer. The United States accounts for 30% of the global NO_x source from fossil fuel combustion [*Benkovitz et al.*, 1996]. We use a continental-scale version of a global three-dimensional (3-D) model of tropospheric photochemistry (cf. *Wang et al.*, 1997a, b, c). We include in our model a relatively detailed treatment of NMHC chemistry and examine the ability of the model to simulate observations for ozone, NO_y species, and photochemical tracers over the United States and Canada. We investigate how uncertainties in NMHC oxidation pathways and other aspects of continental boundary layer chemistry affect the simulation and assess the ability of global models to quantify the export of NO_y species from the continental boundary layer. A companion study by *Liang et al.* [this issue] extends our summertime analysis to investigate the export of NO_y species and ozone from the United States in different seasons.

Of particular importance for our analysis is the chemistry of the highly reactive hydrocarbon isoprene (2-methyl butadiene) emitted by vegetation [*Guenther et al.*, 1995]. Isoprene dominates over anthropogenic NMHCs as a precursor for ozone production over the United States in summer [*Trainer et al.*, 1987, 1991; *Cantrell et al.*, 1993; *Chameides et al.*, 1988, 1992; *McKeen et al.*, 1997]. Atmospheric oxidation of isoprene in the presence of NO_x produces a variety of organic nitrates including PAN and related com-

[1]Now at Advanced Study Program, National Center for Atmospheric Research, Boulder, Colorado.

[2]Now at Department of Civil and Environmental Engineering, Stanford University, Stanford, California.

Copyright 1998 by the American Geophysical Union.

Paper number 97JD03142.
0148-0227/98/97JD-03142$09.00

pounds [*Paulson and Seinfeld*, 1992; *Fehsenfeld et al.*, 1992]. The presence of isoprene also slows down the oxidation of NO_x to HNO_3 by providing a sink for OH radicals in the daytime and a sink for NO_3 at night [*Fan et al.*, 1994].

The model is described in section 2, and a more specific description of the chemical mechanism is given in section 3. We present in section 4 a detailed comparison of model results with observations over the United States and examine the constraints placed by these comparisons on the chemistry of the boundary layer. The export of NO_x and its reservoir species from the U.S. boundary layer is discussed in section 5, and the sensitivity of this export to NMHC chemistry is analyzed in section 6. Conclusions are in section 7.

2. Model Description

This study is performed using a continental-scale version of a global three-dimensional chemical tracer model (CTM). The model is based on that used by *Jacob et al.* [1993b] with substantial improvements. It uses a grid of 4° (latitude) × 5° (longitude) in the horizontal and has nine layers in the vertical defined by a sigma (terrain-following) coordinate. A subgrid nested scheme [*Sillman et al.*, 1990] is used to account for chemical nonlincarities in urban and power plant plumes, as described by Jacob *et al.* [1993b]. The domain includes North America and large areas of the surrounding oceans (see Figure 1). Meteorological input is provided by a general circulation model (GCM) developed at the Goddard Institute for Space Studies (GISS) [*Hansen et al.*, 1983].

The model includes a detailed photochemical mechanism, which is integrated numerically using a modified-Gear algorithm [*Jacobson and Turco*, 1994]. The mechanism includes 80 chemical species, of which 21 species (or families) are transported in the model. A detailed description of the chemistry in the model is provided in section 3. Photolysis rates are calculated hourly using a six-stream radiative transfer routine [*Logan et al.*, 1981], based on albedo and cloud cover from the GCM, and climatological ozone profiles [*Spivakovsky et al.*, 1990].

Emissions of anthropogenic NO_x, CO, and NMHCs are based on national estimates for 1990 for the United States [*Environmental Protection Agency (EPA)*, 1995] and Canada [*Environment Canada*, 1995], with spatial distributions from the National Acid Precipitation Assessment Program (NAPAP) [*EPA*, 1989]. The total emissions used in the model for the United States (based on *EPA* [1995]) represent an increase from the NAPAP totals of 13% for NO_x, 70% for CO, and 10% for NMHCs. Anthropogenic emissions of NO_x, CO, and NMHCs in Central and South America are taken from *Benkovitz et al.* [1996], J. A. Logan (personal communication, 1997), and *Piccot et al.* [1992], respectively. Biogenic emissions of isoprene are calculated based on local vegetation type, temperature, and sunlight, using the algorithm of *Guenther et al.* [1995] as modified by *Wang et al.* [1997a]. The isoprene emissions for the United States in our model (Figure 2) are consistent with those of *Guenther et al.* [1995], and are about a factor of 5 higher than the older estimate by *Lamb et al.* [1987] which has been used in a number of previous O_3 models [e.g., *McKeen et al.*, 1991a, b; *Jacob et al.*, 1993a, b). Biogenic emissions of alkenes and acetone are estimated by scaling to isoprene emissions, based on work by *Goldstein et al.* [1996] and *Singh et al.* [1994a]. The emission ratios used are 0.051 atoms C (alkenes)/atom C (isoprene) and 0.015 molecules acetone/atom C (isoprene).

Advection of tracers in the model is calculated using the second-order moment scheme [*Prather*, 1986]. Dry and wet convective transport of tracers is computed hourly, using convective mass fluxes from the GCM with 4-hour resolution and including a diurnally varying mixed layer [*Prather et al.*, 1987; *Jacob and Prather*, 1990]. Dry deposition velocities for O_3, HNO_3, NO_2, CH_2O, H_2O_2, PAN, and other organic nitrates are computed as described by *Jacob et al.* [1993b] using a resistance-in-series model [*Wesely*, 1989] and local CTM values for surface and environmental variables. The deposition velocities for O_3 and NO_y in our model are in general agreement with observed values at Harvard Forest, Massachusetts [*Munger et al.*, 1996]. Wet deposition of soluble tracers (HNO_3, H_2O_2, and organic hydroxynitrates) is performed using the method developed by *Balkanski et al.* [1993].

The simulations are conducted from May 16 to August 31, with the period May 16–31 used for initialization. We verified that the 16 day initialization period is sufficiently long to ventilate the model domain. Boundary conditions for O_3 at the edges of the model domain (see Figure 1) are specified from ozonesonde data as a function of latitude, altitude, and month [*Logan*, 1994]. Boundary conditions for CO are specified from a global 3-D model study, the results of which are in good agreement with observations (J. A. Logan, personal communication, 1997).

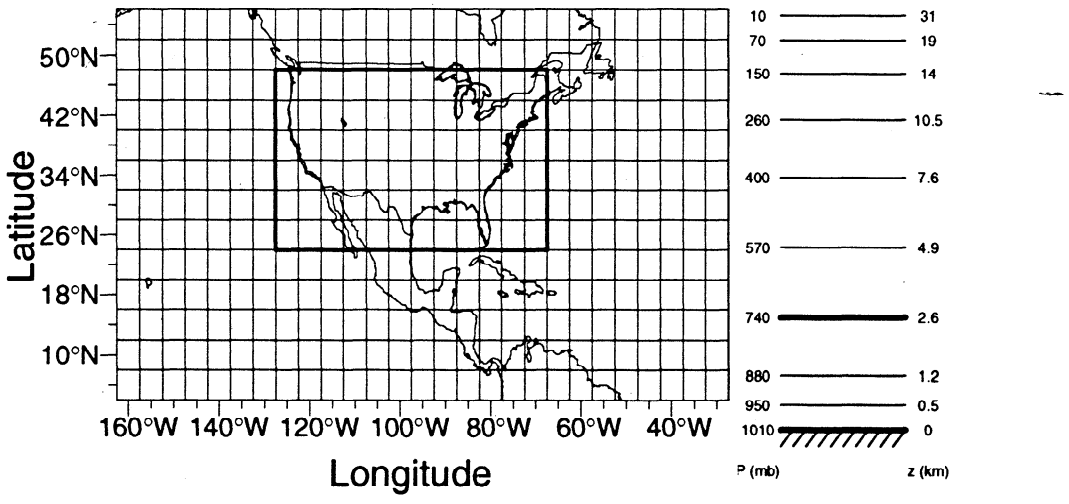

Figure 1. Model domain and grid. The vertical grid is defined by a sigma-coordinate and is shown here for an atmospheric column based at sea level. The heavy line delineates the U.S. boundary layer region used in section 5.

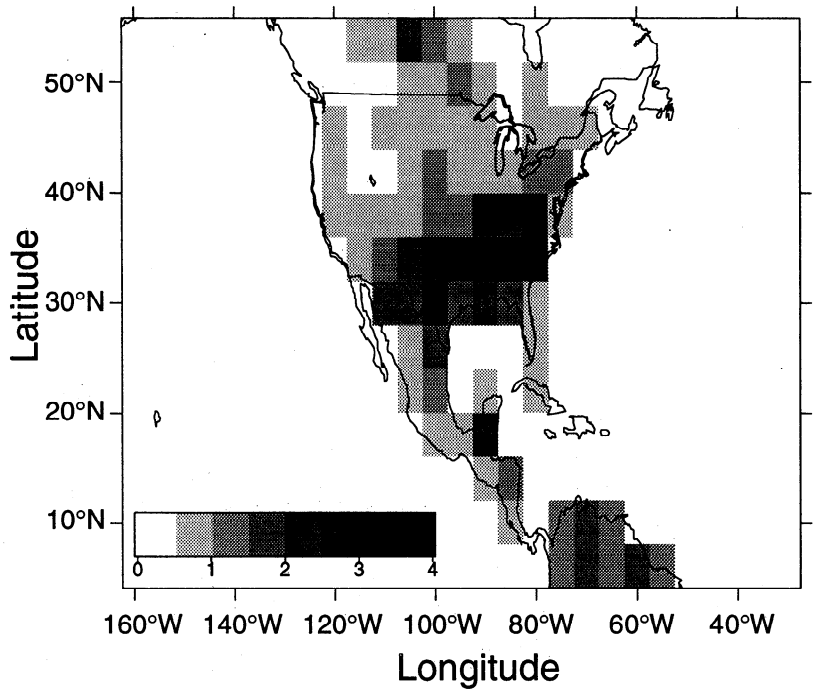

Figure 2. The average biogenic emission source of isoprene in June-August in the model. Units are 10^{12} atoms C cm^{-2} s^{-1}.

Boundary conditions for other tracers are specified as a function of latitude and altitude, using data from the Pacific Exploratory Mission–West Phase A (PEM-West A) aircraft campaign over the North Pacific [*Hoell et al.*, 1996].

3. Chemical Mechanism

3.1. General Chemistry

The chemical mechanism used in our model includes detailed photooxidation schemes for four NMHCs: propane, butane, propene, and isoprene. Butane is used as a surrogate for all alkanes ≥C4, while propene is used to represent all alkenes ≥C3. The lumping for butane and propene is done on a per atom carbon basis, taking advantage of the similarity among the lumped hydrocarbons in the yields (per atom carbon) of ozone, HO_x radicals ($OH+HO_2+RO_2$), and peroxyacyl nitrates (PANs = PAN + higher analogs) [*Jacob et al.*, 1989]. Explicit mechanisms are also included for oxidation of methane and ethane, both of which are present at fixed concentrations in the model (1.7 ppmv and 2.0 ppbv, respectively). Although ethane has variable concentrations over the United States [*Goldstein et al.*, 1995], its contribution to ozone and HO_x chemistry is small [*Cantrell et al.*, 1993; *McKeen et al.*, 1997] so that the assumption of a fixed concentration introduces no significant error. Sensitivity simulations conducted in our model indicate that aromatic hydrocarbons play a negligible role in ozone and HO_x chemistry on a regional scale, in agreement with previous studies of rural photochemistry [*Trainer et al.*, 1991; *Cantrell et al.*, 1993; *McKeen et al.*, 1997]; they are neglected in our mechanism. Biogenic terpenes are also neglected; their chemistry is uncertain, but their effect on O_3 is certainly much less than that of isoprene [*Fehsenfeld et al.*, 1992].

Tracers transported in the model (Table 1) include seven reactive nitrogen species: NO_x, HNO_3, three peroxyacyl nitrates (PAN, PMN, and PPN), a lumped organic hydroxynitrate produced from oxidation of isoprene, and a lumped alkyl nitrate. Also transported in the model are CO, H_2O_2, and the odd oxygen family (O_x) consisting mainly of ozone. Carbonyls produced as intermediates in the oxidation of hydrocarbons (and also directly emitted, in the case of acetone) are represented by seven tracers: formaldehyde, acetaldehyde, methacrolein, other aldehydes (RCHO), acetone, methylvinyl ketone, and other ketones (MEK).

The inorganic and methane photochemistry in our mechanism is based on *DeMore et al.* [1994]. It includes heterogeneous conversion of N_2O_5 and NO_3 to nitric acid in sulfate aerosols, with aerosol surface areas derived from a sulfate simulation using our CTM [*Chin et al.*, 1996; *Liang et al.*, this issue]. A reaction probability γ=0.1 is adopted for these heterogeneous reactions [*DeMore et al.*, 1994]; at aerosol loadings typical of the United States, the rate-limiting step in the heterogeneous conversion to HNO_3 is the nighttime reaction of NO_2 with O_3. Aqueous-phase cloud chemistry appears to have a negligible effect on O_3 and NO_x [*Liang and Jacob*, 1997] and is not included in our simulation.

The chemical mechanism for NMHCs is based on *Atkinson et al.* [1992], except for the isoprene chemistry which is described in the following section. The rates of many reactions have not been studied directly, particularly those involving organic peroxy radicals (RO_2). For these reactions, rate constants are estimated on the basis of similar reactions for which rates have been determined. In our mechanism, we choose a rate constant for the generic RO_2+NO reaction of $k=2.2\times10^{-12}\exp(180/T)$ for all peroxy radicals ≥C3 (except acyl peroxy radicals). This value, based on the measured rates and recommendations of *Kirchner and Stockwell* [1996], is about a factor of 2 slower than the rate for $C_2H_5O_2+NO$. For the RO_2+HO_2 reactions, the rate constant for larger peroxy radicals has been found to be greater than it is for methyl or ethyl peroxy radicals [*Rowley et al.*, 1992]. We adopt the value of *Rowley et al.* [1992], $k=1.4\times10^{-13}\exp(1380/T)$, as our generic RO_2+HO_2 rate for peroxy radicals ≥C3 (except acyl peroxy radicals). This value is approximately a factor of 2.5 times faster than the reactions rates of methyl or ethyl peroxy with HO_2. Many pre-

Table 1. Chemical Tracers in the Model

Tracer	Description
1	$NO_x = NO+NO_2+NO_3+2\times N_2O_5+ HNO_2+HNO_4$
2	$O_x = O_3+O+NO_2+2\times NO_3+3\times N_2O_5+HNO_4$
3	PAN (peroxyacetyl nitrate)
4	HNO_3
5	PMN (peroxymethacryloyl nitrate)
6	PPN (lumped peroxyacyl nitrate)[a]
7	ISN2 (lumped organic hydroxynitrates derived from isoprene)[b]
8	R4N2 (lumped alkyl nitrate)[c]
9	CO
10	H_2O_2
11	Propane
12	ALK4 (lumped alkane ≥C4)[d]
13	PRPE (lumped alkene ≥C3)[e]
14	Isoprene
15	Formaldehyde (CH_2O)
16	Acetaldehyde (CH_3CHO)
17	RCHO (lumped aldehyde ≥C3)[f]
18	Acetone
19	MEK (lumped ketone ≥C4)[g]
20	Methylvinyl ketone
21	Methacrolein

[a]Assumed to have the reactivity of peroxypropionyl nitrate.
[b]Assumed to have reactivity based on a weighted average of "ISN11" and "ISN12" in the work of *Paulson and Seinfeld* [1992]. See Table 2b for details.
[c]Assumed to have the reactivity of butyl nitrate.
[d]Assumed to have a reactivity based on a weighted average of butanes and pentanes [*Lurmann et al.*, 1986].
[e]Assumed to have the reactivity of propene.
[f]Assumed to have the reactivity of propionaldehyde (propanal).
[g]Assumed to have the reactivity of methylethylketone (butanone).

vious photochemical mechanisms have used rates for RO_2+NO and RO_2+HO_2 reactions based on those measured for methyl or ethyl peroxy [*Carter*, 1990; *Stockwell et al.*, 1990]. The rates used in our work result in a higher branching ratio for the RO_2+HO_2 reaction relative to RO_2+NO. Observed HO_2/OH and RO_2/HO_2 ratios from a recent field study in Colorado indicate that larger peroxy radicals must have a lower RO_2+NO rate constant and a higher RO_2+HO_2 rate constant, compared to the values for methyl peroxy radicals [*Stevens et al.*, 1997].

Permutation reactions of organic peroxy radicals with the methyl peroxy radical (CH_3O_2) and the acetyl peroxy radical (CH_3CO_3) are also included in our model. Rates for CH_3O_2+RO_2 reactions are based on *Atkinson* [1994], while those for CH_3CO_3+RO_2 are set equal to the rate for CH_3CO_3+CH_3O_2. Reactions among secondary and tertiary RO_2 radicals have been found to be very slow [*Atkinson*, 1994] and may be neglected. Permutation reactions of primary RO_2 radicals or peroxyacyl radicals not involving either CH_3O_2 or CH_3CO_3 are of minor importance in the atmosphere [*Stockwell et al.*, 1995] and are neglected.

The hydroperoxy radical (HO_2) is highly soluble in aqueous aerosol [*Schwartz*, 1984] where it reacts rapidly with transition metal ions such as Cu(I)/Cu(II) [*Graedel et al.*, 1986; *Mozurkewich et al.*, 1987] and perhaps other species including itself [*Hanson et al.*, 1992]. A model study by *Ross and Noone* [1991] suggests that loss of HO_2 to aqueous aerosol is sufficiently fast to compete with the sink from gas-phase reactions. *Plummer et al.* [1996] found that HO_2 concentrations measured at a nonurban site in Ontario were 2.5 times lower than values derived from a gas-phase model and reported that a missing sink for HO_2 with a corresponding lifetime of 50 s is needed to resolve the discrepancy. Similarly, *Cantrell et al.* [1996] found that adding an aerosol loss for HO_2 to their gas-phase model, with a reaction probability γ=0.5–1.0, greatly improved their agreement with observations at Mauna Loa, Hawaii. As discussed below, our model with gas-phase chemistry only also appears to generate excessive HO_2 concentrations. We include therefore in our standard simulation an aerosol loss of HO_2, using the same sulfate aerosol surface area as used for N_2O_5 and NO_3 and assuming a reaction probability γ=1. No accounting is made of the reaction products; that is, they are assumed inert. The resulting lifetime for HO_2 against scavenging by aerosols is about a minute in surface air over the eastern United States; the effect on model results is discussed in section 4. Organic peroxy radicals RO_2 may be expected in general to have a slower loss to aerosols than HO_2 because they are less water-soluble. We choose not to include aerosol uptake of RO_2 in our standard mechanism but discuss in section 4 the results of a sensitivity simulation including the uptake.

3.2. Isoprene Chemistry

Our mechanism for the oxidation of isoprene is listed in Tables 2a-2c; this mechanism is of particular importance in our study. Several recent studies have determined many of the important features of isoprene oxidation and have produced mechanisms that reasonably simulate observations in chamber studies [*Tuazon and Atkinson*, 1990a; *Paulson and Seinfeld*, 1992; *Carter and Atkinson*, 1996]. The isoprene mechanism used in this work is based upon that of *Paulson and Seinfeld* [1992] but includes a number of modifications.

The main sinks for isoprene are reaction with OH, O_3, and NO_3. The dominant sink is reaction with OH. Reaction of OH with isoprene proceeds by addition of OH to one of the two double bonds, followed by addition of oxygen, producing six different unsaturated peroxy radicals (RO_2), represented in our mechanism as the lumped species RIO2. The principal branch of the RIO2+NO reaction produces alkoxy radicals, which subsequently react with O_2 or decompose to yield the observed products methacrolein (MACR), methylvinyl ketone (MVK), formaldehyde (CH_2O), HO_2, and other carbonyl compounds (IALD). Methacrolein and methylvinyl ketone go on to react with OH and ozone [*Tuazon and Atkinson*, 1989, 1990b; *Paulson and Seinfeld*, 1992] and also photolyze [*Raber and Moortgat*, 1995].

Unsaturated hydroxynitrates denoted ISN2 in our model are formed from RIO2+NO [*Trainer et al.*, 1991], with a yield of about 12% (based on *Atkinson* [1994]). This yield is similar to the value used by *Paulson and Seinfeld* [1992] and somewhat higher than the best fit value of 8.8% found by *Carter and Atkinson* [1996]. Chemical loss of ISN2 is by reaction with OH and ozone, and by photolysis. As in the work of *Paulson and Seinfeld* [1992], we choose rates for the reactions of ISN2 by analogy to the reactions of the structurally similar compounds methacrolein and methylvinyl ketone. We use rate constants of

$k(ISN2+OH)=1.25\times10^{-11}$ and $k(ISN2+O_3)=2.25\times10^{-18}$ cm^3 $molecule^{-1}$ s^{-1}. These reactions result in the return of NO_x to the atmosphere. Photolysis cross sections and quantum yields for ISN2 are assumed to be the same as those measured for methyl nitrate [*Roberts and Fajer*, 1989]. While alkyl nitrates have been found to be rather insoluble and to deposit only slowly to the surface [*Luke et al.*, 1989; *Roberts*, 1990], it is expected that hydroxynitrates such as ISN2 have considerably larger Henry's law constants [*Kames and Schurath*, 1992; *Shepson et al.*, 1996] and hence are more readily deposited [*Roberts*, 1990; *Muthuramu et al.*, 1993]. Further support for rapid deposition of multifunctional organic nitrates is the lack of detection of these species in the ambient atmosphere, although this may possibly be due to rapid chemical removal or to sampling problems [*Muthuramu et al.*, 1993]. We remove ISN2 by dry deposition in our model, with a deposition velocity equal to that of nitric acid as was assumed previously by *Trainer et al.* [1991]; we also scavenge ISN2 in precipitation by assuming that it behaves as a highly soluble tracer.

The reaction of RIO2 with HO_2 produces a hydroxy organic peroxide (denoted RIP in our model). We assume that RIP and all other organic peroxides either react with OH or photolyze with the same rate constants as for CH_3OOH. Alkyl peroxides, which are weak oxidants and sparingly soluble in water [*O'Sullivan et al.*, 1996], are not removed by dry deposition in our model. The presence of a hydroxy group increases the Henry's law constant by 3–4 orders of magnitude [*Zhou and Lee*, 1992; *O'Sullivan et al.*, 1996], allowing efficient scavenging by both wet and dry deposition. Therefore we include a deposition sink for hydroxy organic peroxides in all model grid boxes, with a lifetime of 12 hours, to simulate the effects of dry and wet deposition.

The reaction of isoprene with ozone proceeds by addition of the ozone molecule to either of the double bonds in isoprene, forming a five-membered ring [*Lloyd et al.*, 1983]. The ringed intermediate decomposes forming products including Criegee biradicals. There has been significant disagreement concerning the product yields [*Paulson et al.*, 1992; *Grosjean et al.*, 1993c; *Aschmann and Atkinson*, 1994]. In this work, we adopt the yields recommended by *Aschmann and Atkinson* [1994], which are in reasonably good agreement with those of *Grosjean et al.* [1993c].

Another loss process for isoprene in the model is reaction with the nitrate radical NO_3. While the details of this pathway are fairly uncertain, it is assumed to begin with addition of NO_3 to either of the double bonds. The resulting isoprene-NO_3 adduct reacts with O_2 forming a peroxy radical containing a $-ONO_2$ substituent. We assume that this peroxy radical can react with NO, HO_2, or other peroxy radicals. The product distribution for the NO reaction is from *Paulson and Seinfeld* [1992].

4. Comparison With Observations

4.1. Approach

We evaluate the model results by comparison with measured trace gas concentrations from rural sites in North America, focusing on early afternoon (1300–1600 local time) when surface concentrations are representative of a generally deep mixed layer which can be resolved by the model. Because our model is intended to simulate a typical meteorological year, rather than a specific year, the comparison must be based on seasonal statistics of concentrations. The seasonal median is a particularly useful statistic as it is relatively insensitive to bias by occasional pollution events. When median observations are not available, we use seasonal mean concentrations for comparison. In calculating the median (or mean) model concentrations for a rural site, appropriate area weighting of the rural box and the subgrid plume boxes is done so that the model time series includes representative sampling of aged pollution plumes [*Jacob et al.*, 1993b]. The observations used for comparison are for 1975–1995, while the model emissions are for 1990. There have been no significant long-term trends in rural O_3 concentrations over the United States during the 1975–1995 period [*National Research Council*, 1991; *EPA*, 1993; *Fiore et al.*, 1997]. Emissions of NO_x and volatile organic compounds (VOC) have shown little change from 1975 to 1995, while emissions of CO have declined by about 20% [*EPA*, 1995].

The evaluation for ozone is based on the ensemble of observations from the EPA Aeronometric Information Retrieval System (AIRS), which includes hourly data from hundreds of stations in the United States for the years 1980–1995. The spatial distribution and long-term trends of ozone in the EPA/AIRS record have been described previously by our group [*Fiore et al.*, 1997]. For comparison to our model, the EPA/AIRS record was analyzed to provide median summer afternoon ozone concentrations for each 4°×5° model grid square. These values were obtained by computing the median 1300–1600 LT June–August concentration for each station in a grid square for each year from 1980–1995 and averaging the medians over all stations in the grid square and then over all years. No distinction between urban and nonurban stations was made in the averaging, as we found no significant differences between ozone at these two station categories over the scale of a 4°×5° grid square. For species other than ozone, the observational database in rural air is sparse, and we use for model evaluation an array of measured seasonal statistics assembled from a number of individual investigators (Table 3).

4.2. Ozone

The modeled and observed summer afternoon median concentrations of ozone in surface air (Figures 3a and 3b) show maxima in the eastern United States and southern California, reflecting the distribution of NO_x emissions. The difference between the simulated and observed median ozone concentrations (Figure 3c) shows a region extending from the Gulf of Mexico to Missouri where the model overestimates observations by 20 ppbv or more. The largest overestimate is over Louisiana and eastern Texas, where the model is 30–40 ppbv too high. A scatterplot comparing model and observed median ozone concentrations for each 4°×5° grid square in the United States is shown in Figure 3d. For a majority of the grid boxes, simulated ozone concentrations are within 1 standard deviation of the interannual variability in the observations. Excluding the nine grid points in the south central United States where the model is more than 20 ppbv too high (points marked by crosses), the model concentrations are well-correlated with the observations ($r^2=0.61$), with a linear regression slope of m=1.09. A small overestimate of ozone may be expected as a result of the depositional sink for ozone at the surface, since our model results are for the lowest model layer (0–500 m), while the observations are typically made 10 m above ground.

The overestimate of ozone over the south central United States, which was identified as a problem in an earlier version of this model [*Jacob et al.*, 1993b], appears to be due to a combination of causes. A displacement of the Bermuda High to the northeast in the GISS GCM causes the ventilation of the south central United States with tropical maritime air from the Gulf of Mexico to be too weak [*Jacob and Prather*, 1990]. This circulation problem results in regional stagnation and anomalously high temperatures and insolation, promoting ozone formation. Observational data from

Table 2a. Isoprene Oxidation Mechanism: Chemical Species Involved

Symbol	Formula[a]	Description
ACTA	$CH_3C(O)OH$	acetic acid
ALD2	CH_3CHO	acetaldehyde
CH2O	CH_2O	formaldehyde
CHC	$HCOC(CH_3)(OH)CHO$	carbonyl hydroxy compound and/or dihydroxy compound (assumed inactive)
CO	CO	carbon monoxide
EOH	C_2H_5OH	ethanol
ETO2	CH_3CH_2OO	ethylperoxy radical
ETP	CH_3CH_2OOH	ethylhydroperoxide
GCO3	$HOCH_2C(O)OO$	hydroxy peroxyacetyl radical
GLCO3	$HCOHC(O)OO$	peroxyacyl from GLYX
GLP	$HCOHC(O)OOH$	peroxide from GLCO3
GLPAN	$HCOHC(O)OONO_2$	peroxyacylnitrate from GLCO3
GLYC	$HOCH_2CHO$	glycolaldehyde (hydroxyacetaldehyde)
GLYX	CHOCHO	glyoxal
GP	$HOCH_2C(O)OOH$	peroxide from GCO3
HAC	$HOCH_2C(O)CH_3$	hydroxyacetone
HCOOH	HCOOH	formic acid
IALD	$HOCH_2C(CH_3)=CHCHO$	hydroxy carbonyl alkenes from isoprene
IAO2	$HOCH_2C(CH_3)(OO)CH(OH)CHO$	RO2 from isoprene oxidation products
IAP	$HOCH_2C(CH_3)(OOH)CH(OH)CHO$	peroxide from IAO2
INO2	$O_2NOCH_2C(OO)(CH_3)CH=CH_2$	RO2 from ISOP+NO3
INPN	$O_2NOCH_2C(OOH)(CH_3)CH=CH_2$	peroxide from INO2
ISN1	$HOCH_2C(OO)(CH_3)CH(ONO_2)CH_2OH$	RO2 from ISN2
ISN2	$CH_2=C(CH_3)CH(ONO_2)CH_2OH$	isoprene nitrate
ISNO3	$RONO_2$	stable organic nitrate
ISNP	$HOCH_2C(OOH)(CH_3)CH(ONO_2)CH_2OH$	peroxide from ISN1
ISOP	$CH_2=C(CH_3)CH=CH_2$	isoprene
MACR	$CH_2=C(CH_3)CHO$	methacrolein
MAN2	$HOCH_2C(ONO_2)(CH_3)CHO$	RO2 from MACR+NO3
MAO3	$CH_2=C(CH_3)C(O)OO$	peroxyacyl from MVK and MACR
MAOP	$CH_2=C(CH_3)C(O)OOH$	peroxide from MAO3
MAP	$CH_3C(O)OOH$	peroxyacetic acid
MCO3	$CH_3C(O)OO$	peroxyacetyl radical
MEK	RC(O)R	>C3 ketones
MGLY	CH_3COCHO	methylglyoxal
MNO3	CH_3ONO_2	methylnitrate
MO2	CH_3OO	methylperoxy radical
MOH	CH_3OH	methanol
MRO2	$HOCH_2C(OO)(CH_3)CHO$	RO2 from MACR+OH
MRP	$HOCH_2C(OOH)(CH_3)CHO$	peroxide from MRO2
MVK	$CH_2=CHC(O)CH_3$	methylvinylketone
MVN2	$O_2NOCH_2CH(OO)C(O)CH_3$	RO2 from MVK+NO3
O2CH2OH	O_2CH_2OH	produced by CH2O+HO2

Table 2a. (continued)

Symbol	Formula[a]	Description
PAN	$CH_3C(O)OONO_2$	peroxyacetylnitrate
PMN	$CH_2=C(CH_3)C(O)OONO_2$	peroxymethacryloyl nitrate (MPAN)
PO2	$HOCH_2CH(OO)CH_3$	RO2 from propene
PP	$HOCH_2CH(OOH)CH_3$	peroxide from PO2
PPN	$CH_3CH_2C(O)OONO_2$	peroxypropionylnitrate
PRN1	$O_2NOCH_2CH(OO)CH_3$	RO2 from propene+NO3
PRPE	C_3H_6	propene
PRPN	$O_2NOCH_2CH(OOH)CH_3$	peroxide from PRN1
RCHO	CH_3CH_2CHO	>C2 aldehydes
RCO3	$CH_3CH_2C(O)OO$	peroxypropionyl radical
RCOOH	$C_2H_5C(O)OH$	>C2 organic acids (assumed inactive)
RIO1	$HOCH_2C(OO)(CH_3)CH=CHOH$	RO2 from isoprene oxidation products
RIO2	$HOCH_2C(OO)(CH_3)CH=CH_2$	RO2 from isoprene
RIP	$HOCH_2C(OOH)(CH_3)CH=CH_2$	peroxide from RIO2
ROH	C_3H_7OH	>C2 alcohols
RP	$CH_3CH_2C(O)OOH$	peroxide from RCO3
VRO2	$HOCH_2CH(OO)C(O)CH_3$	RO2 from MVK+OH
VRP	$HOCH_2CH(OOH)C(O)CH_3$	peroxide from VRO2

[a]For lumped species, a sample formula is given.

the EPA/AIRS network show that while median ozone concentrations in the south central United States are relatively low, due to ventilation from the Gulf of Mexico, 90th percentile concentrations are comparable to the northeastern United States [*Fiore et al.*, 1997], indicating the large impact on ozone that can result when ventilation is shut off. An additional cause for our model overestimate of ozone formation in the south central United States may be that we do not have the resolution necessary to simulate the nonlinear chemistry associated with mixing of clean air from the Gulf, large industrial (point) sources of NO_x along the Gulf coast, and high isoprene emission inland.

4.3. NO_y Species

Simulated concentrations of NO_x, PAN, and HNO_3 are compared to observations in Figure 4. The model reproduces observed NO_x values generally to within 30% and also captures the observed spatial gradients. The short chemical lifetime of NO_x (less than a day) against oxidation to HNO_3 causes the concentrations of NO_x to fall off rapidly away from its source regions.

Concentrations of PAN in the model are highest over the northeastern United States, reflecting a combination of high NO_x emissions and relatively low temperatures. Model results are highly correlated with observations but are generally about 30% too low. Our simulation of PAN represents a major improvement over the results of *Jacob et al.* [1993b], where PAN concentrations were overestimated by a factor of 2–3. There are several reasons why our model achieves a better simulation. First, it resolves PAN and the higher peroxyacyl nitrates as separate tracers, whereas these were lumped in the previous study. As discussed below, we find that the higher peroxyacyl nitrates are approximately half as abundant as PAN over the United States. Second, the chemical mechanism used in the earlier study [*Lurmann et al.*, 1986] had an excessive yield of CH_3CO_3 radicals and, consequently, of PAN from isoprene oxidation. This has been corrected in our mechanism, both by the lower yield of methylglyoxal from isoprene and by the inclusion of permutation reactions of CH_3CO_3 radicals with other peroxy radicals. In section 6 we will demonstrate the dominant contribution of isoprene oxidation to the production of PAN.

Simulated concentrations of HNO_3 exceed observations by approximately 25%. This may be expected since model results are for the 0–500 m vertical column, while the observations are near the surface. Because of its rapid dry deposition to the surface, HNO_3 should exhibit a strong vertical gradient in the lowest 500 m of the atmosphere. In addition, the model does not distinguish between gas-phase HNO_3 (g) and aerosol nitrate (NO_3^-), while the observations are for HNO_3 (g) only. Observations indicate that the ratio of NO_3^- to HNO_3 (g) in rural surface air over eastern North America is in the range 0.1–0.4 [*Parrish et al.*, 1993a].

The observed partitioning of NO_y at rural sites [*Parrish et al.*, 1993a; *Munger et al.*, 1996] offers an additional test of NO_y chemistry in the model. Results are shown in Table 4. The simulated ratios agree with observations to within 20%, with the exception of the NO_x/NO_y ratio at Egbert, Ontario, where the observed ratio is much higher than at the other sites; *Parrish et al.* [1993a] note that the NO_x measurements at Egbert may have been biased upward.

4.4. Other Tracers

Simulated and observed concentrations of CO, CH_2O, and H_2O_2 are compared in Figure 5. Elevated concentrations of CO are due to both direct emissions and photochemical production from hydrocarbons, most importantly isoprene. Concentrations of CO are highest over the eastern United States. The model tends to underestimate CO concentrations at most locations by about 15 ppbv.

Table 2b. Isoprene Oxidation Mechanism: Chemical Reactions

Reaction	Rate Constant	Reference
	Reactions With OH	
ISOP+OH=RIO2	2.54E-11 exp(410/T)	3
MVK+OH=VRO2	4.13E-12 exp(452/T)	3, 9
MACR+OH=.5×MAO3+.5×MRO2	1.86E-11 exp(175/T)	3, 9
ALD2+OH=MCO3+H2O	5.60E-12 exp(310/T)	3
RCHO+OH=RCO3+H2O	2.00E-11	3
GLYC+OH=.8×GCO3+.2×GLYX+.2×HO2	1.00E-11	3
GLYX+OH=HO2+2×CO	$1.10E\text{-}11\left(\frac{[O_2]+3.5E18}{2[O_2]+3.5E18}\right)$	3
GLYX+OH=GLCO3	$1.10E\text{-}11\left(\frac{[O_2]}{2[O_2]+3.5E18}\right)$	3
MGLY+OH=MCO3+CO	1.70E-11	3
HAC+OH=MGLY+HO2	3.00E-12	3
IALD+OH=.44×IAO2+.41×MAO3+.15×HO2+.15×CHC	3.70E-11	4
ISN2+OH=ISN1	1.25E-11	2, 4
PRPE+OH=PO2	$k_0 = 8.00E\text{-}27\ (T/300)^{-3.5}$ $k_\infty = 3.00E\text{-}11$ $F = 0.5$	3
ACTA+OH=MO2+CO2+H2O	4.00E-13 exp(200/T)	1
HCOOH+OH=H2O+CO2+HO2	4.00E-13	1
MNO3+OH=CH2O+NO2	3.50E-13	3
MOH+OH=HO2+CH2O	6.70E-12 exp(-600/T)	1
EOH+OH=HO2+ALD2	6.18E-18 exp(532/T)	3
ROH+OH=HO2+RCHO	5.5E-12	3 (1-butanol)
	Reactions With O_3	
ISOP+O3=.387×MACR+.159×MVK+.1×O3+.27×OH+.07×PRPE+.9×CH2O+.06×HO2+.15×CO2+.05×CO+PRODUCTS	1.05E-14 exp(-2000/T)	4, 5
MVK+O3=.82×MGLY+.8×CH2O+.2×O3+.05×CO+.06×HO2+.04×ALD2+.08×OH+PRODUCTS	4.00E-15 exp(-2000/T)	4
MACR+O3=.8×MGLY+.7×CH2O+.2×O3+.2×CO+.275×HO2+.215×OH+.16×CO2+PRODUCTS	4.40E-15 exp(-2500/T)	4
IALD+O3=.6×MGLY+.1×OH+.12×CH2O+.28×GLYC+.3×O3+.2×GLYX+.2×HAC+.2×HCOOH+PRODUCTS	6.16E-15 exp(-1814/T)	4
ISN2+O3=.2×O3+.08×OH+.5×CH2O+.5×IALD+.5×NO2+.5×ISN2	2.25E-18	2, 4
PRPE+O3=.535×CH2O+.5×ALD2+.42×CO+.3×HO2+.135×OH+.065×H2+.305×MO2+PRODUCTS	6.50E-15 exp(-1880/T)	3
	Reactions With NO_3	
ISOP+NO3=INO2	3.03E-12 exp(-446/T)	3
MVK+NO3=MVN2	2.00E-14	2, 11
MACR+NO3=MAN2	6.70E-15	11
MACR+NO3=MAO3+HNO3	3.30E-15	11
ALD2+NO3=HNO3+MCO3	1.40E-12 exp(-1860/T)	3
RCHO+NO3=HNO3+RCO3	1.40E-12 exp(-1860/T)	3 (ALD2)

Table 2b. (continued)

Reaction	Rate Constant	Reference
RCHO+NO3=HNO3+RCO3	1.40E-12 exp(-1860/T)	3 (ALD2)
GLYX+NO3=HNO3+HO2+2×CO	$1.40E\text{-}12\ \exp(-1860/T) \times \left(\frac{[O_2] + 3.5E18}{2[O_2] + 3.5E18}\right)$	3 (ALD2)
GLYX+NO3=HNO3+GLCO3	$1.40E\text{-}12\ \exp(-1860/T) \times \left(\frac{[O_2]}{2[O_2] + 3.5E18}\right)$	3 (ALD2)
MGLY+NO3=HNO3+CO+MCO3	1.40E-12 exp(-1860/T)	3 (ALD2)
PRPE+NO3=PRN1	4.59E-13 exp(-1156/T)	3
Reactions Involving PANs		
MCO3+NO2=PAN	$k_0 = 2.7E\text{-}28\ (T/300)^{-7.1}$ $k_\infty = 1.2E\text{-}11\ (T/300)^{-0.9}$ F = 0.3	3[a]
RCO3+NO2=PPN	$1.20E\text{-}11\ (T/300)^{-0.9}$	3
GCO3+NO2=GPAN	$1.20E\text{-}11\ (T/300)^{-0.9}$	3
MAO3+NO2=PMN	$1.20E\text{-}11\ (T/300)^{-0.9}$	3
GLCO3+NO2=GLPAN	$1.20E\text{-}11\ (T/300)^{-0.9}$	3
PAN=MCO3+NO2	$k_0 = 4.9E\text{-}03\ \exp(-12100/T)$ $k_\infty = 4.0E+16\ \exp(-13600/T)$ F = 0.3	3[a]
PPN=RCO3+NO2	4.00E+16 exp(-13600/T)	3
GPAN=GCO3+NO2	4.00E+16 exp(-13600/T)	3
PMN=MAO3+NO2	4.00E+16 exp(-13600/T)	3
GLPAN=GLCO3+NO2	4.00E+16 exp(-13600/T)	3
PAN=MNO3+CO2	2.10E+12 exp(-12525/T)	12
PMN+OH=NO2+.59×HAC+2×HO2+PRODUCTS	3.60E-12	10
PMN+O3=NO2+.6×CH2O+HO2+PRODUCTS	8.20E-18	10
RO_2+NO Reactions		
ETO2+NO=ALD2+NO2+HO2	4.90E-12 exp(180/T)	3
IAO2+NO=.92×HO2+.27×CO+.17×GLYX+.33×HAC+.24×GLYC+.53×MGLY+.92×NO2+.07×CHC+.08×ISN2	2.20E-12 exp(180/T)	4, 7
INO2+NO=1.1×NO2+.8×HO2+.85×ISN2+.05×NO2+.1×MACR+.15×CH2O+.05×MVK	2.20E-12 exp(180/T)	4, 7
ISN1+NO=1.9×NO2+.95×GLYC+.95×HAC+.05×ISN2+.05×NO2+.05×HO2	2.20E-12 exp(180/T)	2, 4, 7
MAN2+NO=2×NO2+CH2O+MGLY	2.20E-12 exp(180/T)	7
MRO2+NO=NO2+HO2+.17×MGLY+.83×HAC+.83×CO+.17×CH2O	$(1\text{-}f_N)$ 2.20E-12 exp(180/T)	7[b]
MRO2+NO=ISN2	f_N 2.20E-12 exp(180/T)	7[b]
MVN2+NO=1.2×NO2+.3×HO2+.3×CH2O+.6×MCO3+.6×GLYC+.3×MGLY+.8×ISN2	2.20E-12 exp(180/T)	7
PO2+NO=NO2+HO2+CH2O+ALD2	2.20E-12 exp(180/T)	7
PRN1+NO=2×NO2+CH2O+ALD2	2.20E-12 exp(180/T)	7
RIO1+NO=NO2+IALD+HO2+.75×CH2O	$(1\text{-}f_N)$ 2.20E-12 exp(180/T)	4, 7[b]

Table 2b. (continued)

Reaction	Rate Constant	Reference
RIO1+NO=ISN2	f_N 2.20E-12 exp(180/T)	4, 7[b]
RIO2+NO=NO2+.864×HO2+.69×CH2O+.402×MVK+.288×MACR+ .136×RIO1+.127×IALD	(1-f_N) 2.20E-12 exp(180/T)	4, 7[b]
RIO2+NO=ISN2	f_N 2.20E-12 exp(180/T)	4, 7[b]
VRO2+NO=NO2+.28×HO2+.28×CH2O+.72×MCO3+.72×GLYC+ .28×MGLY	(1-f_N) 2.20E-12 exp(180/T)	7[b]
VRO2+NO=ISN2	f_N 2.20E-12 exp(180/T)	7[b]
MCO3+NO=MO2+NO2+CO2	2.00E-11	3
RCO3+NO=NO2+ETO2	2.00E-11	3
GCO3+NO=NO2+HO2+CH2O	2.00E-11	3
MAO3+NO=NO2+CH2O+HO2	2.00E-11	2, 3, 9
GLCO3+NO=NO2+HO2+CO	2.00E-11	2
	RO_2+HO_2 Reactions	
ETO2+HO2=ETP	6.50E-13 exp(650/T)	3
IAO2+HO2=IAP	1.40E-13 exp(1380/T)	8
INO2+HO2=INPN	1.40E-13 exp(1380/T)	8
ISN1+HO2=ISNP	1.40E-13 exp(1380/T)	8
MAN2+HO2=ISNP	1.40E-13 exp(1380/T)	8
MRO2+HO2=MRP	1.40E-13 exp(1380/T)	8
MVN2+HO2=ISNP	1.40E-13 exp(1380/T)	8
PO2+HO2=PP	4.90E-13 exp(720/T)	3
PRN1+HO2=PRPN	1.40E-13 exp(1380/T)	8
RIO1+HO2=RIP	1.40E-13 exp(1380/T)	8
RIO2+HO2=RIP	1.40E-13 exp(1380/T)	8
VRO2+HO2=VRP	1.40E-13 exp(1380/T)	8
MCO3+HO2=ACTA+O3	3.00E-13 exp(1040/T)	3
MCO3+HO2=MAP	1.30E-13 exp(1040/T)	3
RCO3+HO2=.7×RCOOH+.7×O3+.3×RP	4.30E-13 exp(1040/T)	3
GCO3+HO2=.7×RCOOH+.7×O3+.3×GP	4.30E-13 exp(1040/T)	3
MAO3+HO2=.7×RCOOH+.7×O3+.3×MAOP	4.30E-13 exp(1040/T)	3
GLCO3+HO2=.7×RCOOH+.7×O3+.3×GLP	4.30E-13 exp(1040/T)	3
	ROOH+OH Reactions	
ETP+OH=.5×OH+.5×ETO2+.5×ALD2	3.80E-12 exp(200/T)	1 (CH_3OOH+OH)
GP+OH=.5×OH+.5×GCO3+.5×CH2O	3.80E-12 exp(200/T)	1 (CH_3OOH+OH)
GLP+OH=.5×OH+.5×GLCO3+.5×CO	3.80E-12 exp(200/T)	1 (CH_3OOH+OH)
IAP+OH=.5×OH+.5×RCHO+.5×IAO2	3.80E-12 exp(200/T)	1 (CH_3OOH+OH)
INPN+OH=INO2	3.80E-12 exp(200/T)	1 (CH_3OOH+OH)
ISNP+OH=.5×OH+.5×RCHO+.5×NO2+.5×ISN1	3.80E-12 exp(200/T)	1 (CH_3OOH+OH)
MAOP+OH=.5×OH+.5×RCHO+.5×MAO3	3.80E-12 exp(200/T)	1 (CH_3OOH+OH)
MRP+OH=.5×OH+.5×RCHO+.5×MRO2	3.80E-12 exp(200/T)	1 (CH_3OOH+OH)
PP+OH=.5×OH+.5×PO2+.5×RCHO	3.80E-12 exp(200/T)	1 (CH_3OOH+OH)
PRPN+OH=PRN1	3.80E-12 exp(200/T)	1 (CH_3OOH+OH)

Table 2b. (continued)

Reaction	Rate Constant	Reference
RIP+OH=.5×IAO2+.4×RIO2+.1×RIO1	3.80E-12 exp(200/T)	1 (CH_3OOH+OH), 2
VRP+OH=.5×OH+.5×RCHO+.5×VRO2	3.80E-12 exp(200/T)	1 (CH_3OOH+OH)
RO_2+RO_2 Reactions		
ETO2+MO2=.75×CH2O+.75×ALD2+HO2+.25×MOH+.25×EOH	3.00E-13	2, 3
PO2+MO2=HO2+.5×ALD2+1.25×CH2O+.16×HAC+.09×RCHO+ .25×MOH+.25×ROH	6.00E-13	2, 3
RIO2+MO2=.43×HO2+.35×CH2O+.20×MVK+.14×MACR+ .07×RIO1+.06×IALD+.25×MEK+.75×CH2O+.25×MOH+ .25×ROH+.5×HO2	8.00E-14	2, 3
RIO1+MO2=.5×IALD+.5×HO2+.38×CH2O+.25×MEK+.75×CH2O+ .25×MOH+.25×ROH+.5×HO2	8.00E-14	2,3
IAO2+MO2=.5×HO2+.15×CO+.09×GLYX+.18×HAC+.13×GLYC+ .29×MGLY+.04×CHC+.25×MEK+.75×CH2O+.25×MOH+ .25×ROH+.5×HO2	8.00E-14	2,3
ISN1+MO2=NO2+.5×GLYC+.5×HAC+.25×RCHO+.75×CH2O+ .25×MOH+.25×ROH+.5×HO2	8.00E-14	2,3
VRO2+MO2=.14×HO2+.14×CH2O+.36×MCO3+.36×GLYC+ .14×MGLY+.25×MEK+.75×CH2O+.25×MOH+.25×ROH+.5×HO2	8.00E-14	2,3
MRO2+MO2=.5×HO2+.09×MGLY+.42×HAC+.42×CO+.09×CH2O+ .25×MEK+.75×CH2O+.25×MOH+.25×ROH+.5×HO2	8.00E-14	2,3
MVN2+MO2=NO2+.5×CH2O+.25×MCO3+.25×MGLY+.25×HO2+ .25×RCHO+.75×CH2O+.25×MOH+.25×ROH+.5×HO2	8.00E-14	2,3
MAN2+MO2=NO2+.5×CH2O+.5×MGLY+.25×RCHO+.75×CH2O+ .25×MOH+.25×ROH+.5×HO2	8.00E-14	2,3
INO2+MO2=.55×NO2+.4×HO2+.425×ISN2+.025×NO2+.05×MACR+ .08×CH2O+.03×MVK+.25×RCHO+.75×CH2O+.25×MOH+ .25×ROH+.5×HO2	8.00E-14	2,3
PRN1+MO2=NO2+.5×CH2O+.5×ALD2+.25×RCHO+.75×CH2O+ .25×MOH+.25×ROH+.5×HO2	8.00E-14	2,3
ETO2+ETO2=2×ALD2+2×HO2	6.08E-14 exp(-110/T)	3
ETO2+ETO2=EOH+ALD2	3.72E-14 exp(-110/T)	3
MCO3+MO2=CH2O+MO2+HO2	$\frac{1.4E\text{-}11}{1 + 4.55E\text{-}07\exp(3820/T)}$	1
MCO3+MO2=ACTA+CH2O	$\frac{1.4E\text{-}11}{1 + 2.20E+06\exp(-3820/T)}$	1
MCO3+ETO2=MO2+ALD2+HO2	$\frac{1.4E\text{-}11}{1 + 4.55E\text{-}07\exp(3820/T)}$	1, 2
MCO3+ETO2=ACTA+ALD2	$\frac{1.4E\text{-}11}{1 + 2.20E+06\exp(-3820/T)}$	1, 2
MCO3+PO2=MO2+ALD2+CH2O+HO2	$\frac{1.4E\text{-}11}{1 + 4.55E\text{-}07\exp(3820/T)}$	1, 2
MCO3+PO2=ACTA+.35×RCHO+.65×HAC	$\frac{1.4E\text{-}11}{1 + 2.20E+06\exp(-3820/T)}$	1, 2
RCO3+MO2=CH2O+HO2+ETO2	$\frac{1.4E\text{-}11}{1 + 4.55E\text{-}07\exp(3820/T)}$	1, 2

Table 2b. (continued)

Reaction	Rate Constant	Reference
RCO3+MO2=RCOOH+CH2O	$\frac{1.4E\text{-}11}{1 + 2.20E\text{+}06\exp(-3820/T)}$	1, 2
GCO3+MO2=2×CH2O+2×HO2	$\frac{1.4E\text{-}11}{1 + 4.55E\text{-}07\exp(3820/T)}$	1, 2
GCO3+MO2=RCOOH+CH2O	$\frac{1.4E\text{-}11}{1 + 2.20E\text{+}06\exp(-3820/T)}$	1, 2
MAO3+MO2=CH2O+HO2+CH2O+MCO3	$\frac{1.4E\text{-}11}{1 + 4.55E\text{-}07\exp(3820/T)}$	1, 2
MAO3+MO2=RCOOH+CH2O	$\frac{1.4E\text{-}11}{1 + 2.20E\text{+}06\exp(-3820/T)}$	1, 2
GLCO3+MO2=CH2O+2×HO2+CO	$\frac{1.4E\text{-}11}{1 + 4.55E\text{-}07\exp(3820/T)}$	1, 2
GLCO3+MO2=RCOOH+CH2O	$\frac{1.4E\text{-}11}{1 + 2.20E\text{+}06\exp(-3820/T)}$	1, 2
MCO3+MCO3=2×MO2	2.8E-12 exp(530/T)	6
MCO3+RIO2=MO2+.864×HO2+.69×CH2O+.402×MVK+ .288×MACR+.136×RIO1+.127×IALD	$\frac{1.4E\text{-}11}{1 + 4.55E\text{-}07\exp(3820/T)}$	1, 2
MCO3+RIO1=MO2+IALD+HO2+.75×CH2O	$\frac{1.4E\text{-}11}{1 + 4.55E\text{-}07\exp(3820/T)}$	1, 2
MCO3+IAO2=MO2+HO2+.29×CO+.18×GLYX+.36×HAC+ .26×GLYC+.58×MGLY+.08×CHC	$\frac{1.4E\text{-}11}{1 + 4.55E\text{-}07\exp(3820/T)}$	1, 2
MCO3+ISN1=MO2+NO2+GLYC+HAC	$\frac{1.4E\text{-}11}{1 + 4.55E\text{-}07\exp(3820/T)}$	1, 2
MCO3+VRO2=MO2+.28×HO2+.28×CH2O+.72×MCO3+.72×GLYC+ .28×MGLY	$\frac{1.4E\text{-}11}{1 + 4.55E\text{-}07\exp(3820/T)}$	1, 2
MCO3+MRO2=MO2+HO2+.17×MGLY+.83×HAC+.83×CO+ .17×CH2O	$\frac{1.4E\text{-}11}{1 + 4.55E\text{-}07\exp(3820/T)}$	1, 2
MCO3+MVN2=MO2+NO2+CH2O+.5×MCO3+.5×MGLY+.5×HO2	$\frac{1.4E\text{-}11}{1 + 4.55E\text{-}07\exp(3820/T)}$	1, 2
MCO3+MAN2=MO2+NO2+CH2O+MGLY	$\frac{1.4E\text{-}11}{1 + 4.55E\text{-}07\exp(3820/T)}$	1, 2
MCO3+INO2=MO2+.1×NO2+.8×HO2+.85×ISN2+.05×NO2+ .1×MACR+.15×CH2O+.05×MVK	$\frac{1.4E\text{-}11}{1 + 4.55E\text{-}07\exp(3820/T)}$	1, 2
MCO3+RIO2=MEK+ACTA	$\frac{1.4E\text{-}11}{1 + 2.20E\text{+}06\exp(-3820/T)}$	1, 2
MCO3+RIO1=MEK+ACTA	$\frac{1.4E\text{-}11}{1 + 2.20E\text{+}06\exp(-3820/T)}$	1, 2
MCO3+IAO2=MEK+ACTA	$\frac{1.4E\text{-}11}{1 + 2.20E\text{+}06\exp(-3820/T)}$	1, 2
MCO3+ISN1=RCHO+ACTA+NO2	$\frac{1.4E\text{-}11}{1 + 2.20E\text{+}06\exp(-3820/T)}$	1, 2

Table 2b. (continued)

Reaction	Rate Constant	Reference
MCO3+VRO2=MEK+ACTA	$\frac{1.4E\text{-}11}{1 + 2.20E+06\exp(-3820/T)}$	1, 2
MCO3+MRO2=MEK+ACTA	$\frac{1.4E\text{-}11}{1 + 2.20E+06\exp(-3820/T)}$	1, 2
MCO3+MVN2=RCHO+ACTA+NO2	$\frac{1.4E\text{-}11}{1 + 2.20E+06\exp(-3820/T)}$	1, 2
MCO3+MAN2=RCHO+ACTA+NO2	$\frac{1.4E\text{-}11}{1 + 2.20E+06\exp(-3820/T)}$	1, 2
MCO3+INO2=RCHO+ACTA+NO2	$\frac{1.4E\text{-}11}{1 + 2.20E+06\exp(-3820/T)}$	1, 2
MCO3+PRN1=MO2+NO2+CH2O+ALD2	$\frac{1.4E\text{-}11}{1 + 4.55E\text{-}07\exp(3820/T)}$	1, 2
MCO3+PRN1=RCHO+ACTA+NO2	$\frac{1.4E\text{-}11}{1 + 2.20E+06\exp(-3820/T)}$	1, 2
MCO3+RCO3=MO2+ETO2	2.8E-12 exp(530/T)	6
MCO3+GCO3=MO2+HO2+CH2O	2.8E-12 exp(530/T)	6
MCO3+MAO3=MO2+CH2O+MCO3	2.8E-12 exp(530/T)	6
MCO3+GLCO3=MO2+HO2+CO	2.8E-12 exp(530/T)	6

Read 2.54E-11 as 2.54×10^{-11}. Reference code: 1, *DeMore et al.* [1994]; 2, this work; 3, *Atkinson et al.* [1992], *Atkinson* [1994]; 4, *Paulson and Seinfeld* [1992]; 5, *Aschmann and Atkinson* [1994]; 6, *Lightfoot et al.* [1992]; 7, *Kirchner and Stockwell* [1996], 8, *Rowley et al.* [1992]; 9, *Tuazon and Atkinson* [1989, 1990b]; 10, *Grosjean et al.* [1993a b], 11, *Lurmann et al.* [1986]; 12, *Roberts* [1990].

[a] $k = \left(\frac{k_0[M]}{1 + k_0M/k_\infty}\right) \times F^{\{1 + \log_{10}(k_0M/k_\infty)^2\}^{-1}}$

[b] f_N = fractional yield of organic nitrate from reaction of RO_2+NO, computed as a function of temperature and number of carbon atoms [*Atkinson*, 1990].

Photolysis of CH_2O is an important source of HO_x radicals over the United States [*McKeen et al.*, 1991a]. The model matches observed mean or median concentrations to within 10%, except at the Georgia site where it is too high. The dominant source of CH_2O over the United States in the model is oxidation of isoprene, consistent with observations [*Munger et al.*, 1995].

Production of H_2O_2, by the self-reaction of HO_2, is a major sink for HO_x over the United States, so that simulation of H_2O_2 provides a test of HO_x chemistry in the model. Model results show a maximum over the southeastern United States, reflecting high humidities and high isoprene emissions, but overestimate observations by 60–80% at the two sites in that region (F and N). Displacement of the Bermuda High in the model causes reduced precipitation over the southeast United States compared to observations [*Balkanski*, 1991]. As a result, the loss of H_2O_2 by wet deposition is suppressed, contributing to the high concentrations in the model. Another possible reason for the high H_2O_2 concentrations in the model is our neglect of H_2O_2 loss by oxidation of SO_2 in clouds. Using sulfur budgets calculated by *Chin and Jacob* [1996] for the U.S. boundary layer, we find that the in-cloud rate of SO_2 oxidation by H_2O_2 is approximately 60% as large as the rate we calculate for (wet plus dry) deposition of H_2O_2. Thus our neglect of SO_2 oxidation may contribute significantly to the excessive H_2O_2. As mentioned below, results from a sensitivity study indicate that without the aerosol sink for HO_2 included in our model, simulated H_2O_2 concentrations would be considerably higher.

Simulated concentrations of acetaldehyde, methylvinyl ketone, and methacrolein are shown in Figure 6. The available data for these species are rather limited (see Table 3). Model values are generally within 50% of observations. In Kinterbish, Alabama, the model overestimates methacrolein by a factor of 3 and methylvinyl ketone by about 60%. This overestimate may be attributed to high isoprene emissions in the model, resulting from anomalously high temperatures and insolation in the region. In addition, the observations were made above a pine plantation where isoprene emission was presumably less than the regional average. The mean MVK/MACR ratio of afternoon concentrations in our model at Kinterbish is 1.2, significantly lower than the value of about 2–2.5 found by *Montzka et al.* [1995]. The high isoprene emissions (which suppress OH concentrations) and high ozone concentrations in our model increase the importance of reactions of isoprene, methylvinyl ketone, and methacrolein with O_3 relative to those with OH. The O_3 reactions decrease the MVK/MACR ratio compared to the OH reactions.

4.5. Ozone Production Efficiency

Summertime observations at nonurban sites in the eastern United States indicate strong correlations of ozone with CO and with the products of NO_x oxidation (NO_y-NO_x). The slopes ΔO_3/

Table 2c. Isoprene Oxidation Mechanism: Photolysis Reactions

Species	Products	Rate,[a] s^{-1}	Reference
ALD2	MO2+HO2+CO	4.77E-06	3
ALD2	CH4+CO	3.34E-06	3
ETP	OH+HO2+ALD2	5.29E-06	1 (CH_3OOH)
GLP	OH+HO2+CO	5.29E-06	1 (CH3OOH)
GLYC	CH2O+2×HO2+CO	8.11E-06	3 (ALD2)
GLYX	H2+2×CO	5.98E-05	3
GLYX	2×CO+2×HO2	9.60E-06	3
GLYX	CH2O+CO	1.92E-05	3
GP	OH+HO2+CH2O	5.29E-06	1 (CH_3OOH)
HAC	MCO3+CH2O+HO2	6.20E-07	3 (ACET)
IAP	OH+HO2+.29×CO+.19×GLYX+.36×HAC+ .26×GLYC+.58×MGLY	5.29E-06	1 (CH_3OOH), 2
INPN	OH+HO2+RCHO+NO2	5.29E-06	1 (CH_3OOH)
ISN2	NO2+.864×HO2+.69×CH2O+.402×MVK+ .288×MACR+.136×RIO1+.127×IALD	1.51E-06	2, 3 (MNO3)
ISNP	OH+HO2+RCHO+NO2	5.29E-06	1 (CH_3OOH)
MACR	MAO3+HO2	7.48E-06	5
MACR	CO+HO2+.8×MGLY+.8×HO2+.2×MCO3+ .2×CH2O	7.48E-06	5
MAOP	OH+HO2+RCHO	5.29E-06	1 (CH_3OOH)
MAP	OH+MO2	5.29E-06	1 (CH_3OOH)
MGLY	MCO3+CO+HO2	7.42E-04	5
MGLY	ALD2+CO	8.15E-06	5
MNO3	CH2O+H2O+NO2	1.51E-06	3
MRP	OH+HO2+.17×MGLY+.83×HAC+.83×CO+ .17×CH2O	5.29E-06	1 (CH_3OOH), 2
MVK	PRPE+CO	1.49E-05	5
MVK	MCO3+CH2O+CO+HO2	4.98E-06	5
MVK	MO2+MAO3	4.98E-06	5
O3	$O(^1D)$	3.86E-05	1,4
PAN	MCO3+NO2	8.08E-07	6
PP	OH+HO2+RCHO	5.29E-06	1 (CH_3OOH)
RCHO	ETO2+HO2+CO	1.96E-05	3
PRPN	OH+HO2+RCHO+NO2	5.29E-06	1 (CH_3OOH)
RIP	OH+.864×HO2+.69×CH2O+.402×MVK+ .288×MACR+.136×RIO1+.127×IALD	5.29E-06	1 (CH_3OOH), 2
VRP	OH+.28×HO2+.28×CH2O+.72×MCO3+ .72×GLYC+.28×MGLY	5.29E-06	1 (CH_3OOH), 2

Read 4.77E-06 as 4.77×10^{-6}. Reference code: 1, *DeMore et al.* [1994]; 2, this work; 3, *Atkinson et al.* [1992], *Atkinson* [1994]; 4, *Michelson et al.* [1994]; 5, *Raber and Moortgat* [1995]; 6, *Talukdar et al.* [1995].

[a]Photolysis rate constant computed for a point at the surface at a latitude of 42°N at local noon on July 1, assuming clear-sky conditions, a surface albedo of 0.10, an ozone column of 8.061×10^{18} molecules cm^{-2} (300 DU, Dobson unit), and a local temperature of 298 K.

Table 3. Summer (June-August) Observations at Nonurban Sites

Symbol	Site	Location, deg	Years[e]	Concentration (ppbv)	Statistic	Reference
			NO_x			
A	Harvard Forest, Massachusetts	43N, 72W	1990-1995	0.64	1200-1500 LT median	*Munger et al.* [1996]
B	Scotia, Pennsylvania	41N, 78W	1988	1.30	1400 LT median	*Parrish et al.* [1993a]
C	Niwot Ridge, Colorado[a,b]	40N, 105W	1981, 1983, 1984	0.29	median of all data	*Parrish et al.* [1990]
D	Bondville, Illinois	40N, 88W	1988	1.11	1400 LT median	*Parrish et al.* [1993a]
E	Schefferville, Quebec	55N, 67W	1990	0.04	1400 LT median	*Bakwin et al.* [1994]
F	Metter, Georgia	33N, 82W	1991-1992	0.50	1400 LT mean	*Kleinman et al.* [1994, 1995]
G	Egbert, Ontario	44N, 80W	1988	0.95	1400 LT median	*Parrish et al.* [1993a]
H	Mauna Loa, Hawaii[c]	19N, 156W	1992	0.05	mean of free tropospheric observations	*Brasseur et al.* [1996a]
I	Central Piedmont, North Carolina	35N, 80W	1991	0.80	1400 LT mean	*Poulida et al.* [1994]
			PAN			
B	Scotia, Pennsylvania	41N, 78W	1988	1.1	1400 LT mean	*Roberts et al.* [1995]
D	Bondville, Illinois	40N, 88W	1988	1.3	1400 LT mean	*Roberts et al.* [1995]
F	Metter, Georgia	33N, 82W	1991	0.22	daytime mean	*Kleinman et al.* [1994]
G	Egbert, Ontario	44N, 80W	1988	0.70	1400 LT mean	*Roberts et al.* [1995]
I	Central Piedmont, North Carolina	35N, 80W	1992	0.55	1400 LT mean	*Hartsell et al.* [1994]
J	Pride, Louisiana	31N, 91W	1989	0.40	1400 LT median	*Jacob et al.* [1993b]
K	Elberton, Georgia	34N, 83W	1991	0.70	1400 LT median	*Jacob et al.* [1993b]
			HNO_3			
B	Scotia, Pennsylvania	41N, 78W	1988	1.3	1400 LT median	*Parrish et al.* [1993a]
F	Metter, Georgia	33N, 82W	1991	1.0	1400 LT mean	*Kleinman et al.* [1994, 1995]
G	Egbert, Ontario	44N, 80W	1988	0.68	1400 LT median	*Parrish et al.* [1993a]
			CO			
A	Harvard Forest, Massachusetts	43N, 72W	1990-1995	159	1200-1500 LT median	J.W. Munger, unpublished data [1997]
B	Scotia, Pennsylvania	41N, 78W	1988	215	0800-1700 LT mean	*Parrish et al.* [1991]
C	Niwot Ridge, Colorado[a,b]	40N, 105W	1988	117	median of all data	*Parrish et al.* [1991]
F	Metter, Georgia	33N, 82W	1991	213	daytime mean	*Kleinman et al.* [1994]
H	Mauna Loa, Hawaii[c]	19N, 156W	1992	65	median of free tropospheric observations	*Atlas and Ridley* [1996]
I	Central Piedmont, North Carolina	35N, 80W	1991	182	1400 LT mean	*Poulida et al.* [1994]

Table 3. (continued)

Symbol	Site	Location, deg	Years[e]	Concentration (ppbv)	Statistic	Reference
J	Pride, Louisiana	31N, 91W	1989	177	0800-1700 LT median	*Jacob et al.* [1993b]
L	Shenandoah National Park, Virginia[b,d]	39N, 79W	1989	211	median of all data	*Poulida et al.* [1991]
			CH_2O			
B	Scotia, Pennsylvania	41N, 78W	1988	4.4	1400 LT mean	*Martin et al.* [1991]
F	Metter, Georgia	33N, 82W	1991-1992	3.35	midafternoon median	*Lee et al.* [1995]
G	Egbert, Ontario	44N, 80W	1988	2.0	1400 LT mean	*Shepson et al.* [1991]
H	Mauna Loa, Hawaii[c]	19N, 156W	1992	0.15	median of free tropospheric observations	*Atlas and Ridley* [1996]
M	Dorset, Ontario	45N, 79W	1988	2.5	1400 LT mean	*Shepson et al.* [1991]
			H_2O_2			
C	Niwot Ridge, Colorado[a,b]	40N, 105W	1987, 1989	0.8	1400 LT median	*Watkins et al.* [1995a]
F	Metter, Georgia	33N, 82W	1991	1.3	1400 LT mean	*Kleinman et al.* [1994]
H	Mauna Loa, Hawaii[c]	19N, 156W	1992	1.54	median of free tropospheric observations	*Atlas and Ridley* [1996]
N	Kinterbish, Alabama	32N, 88W	1990, 1992	1.6	1400 LT median	*Watkins et al.* [1995b]
			CH_3CHO			
F	Metter, Georgia	33N, 82W	1991	0.66	midafternoon median	*Lee et al.* [1995]
G	Egbert, Ontario	44N, 80W	1988	0.70	1400 LT mean	*Shepson et al.* [1991]
M	Dorset, Ontario	45N, 79W	1988	0.90	1400 LT mean	*Shepson et al.* [1991]
			Methylvinyl Ketone			
B	Scotia, Pennsylvania	41N, 78W	1988	1.6	1400 LT mean	*Martin et al.* [1991]
N	Kinterbish, Alabama	32N, 88W	1990, 1992	1.3	1400 LT mean	*Montzka et al.* [1993, 1995]
			Methacrolein			
B	Scotia, Pennsylvania	41N, 78W	1988	0.90	1400 LT mean	*Martin et al.* [1991]
N	Kinterbish, Alabama	32N, 88W	1990, 1992	0.60	1400 LT mean	*Montzka et al.* [1993, 1995]

[a]Mountain ridge site at 3050 m altitude.
[b]For mountain sites, the model can be evaluated with observations at all times of day.
[c]Mountain site at 3400 m altitude. We evaluate the model by comparison with "free tropospheric" observations [*Atlas and Ridley*, 1996].
[d]Mountain ridge site at 1100 m altitude.
[e]Including at least 1 month of observations.

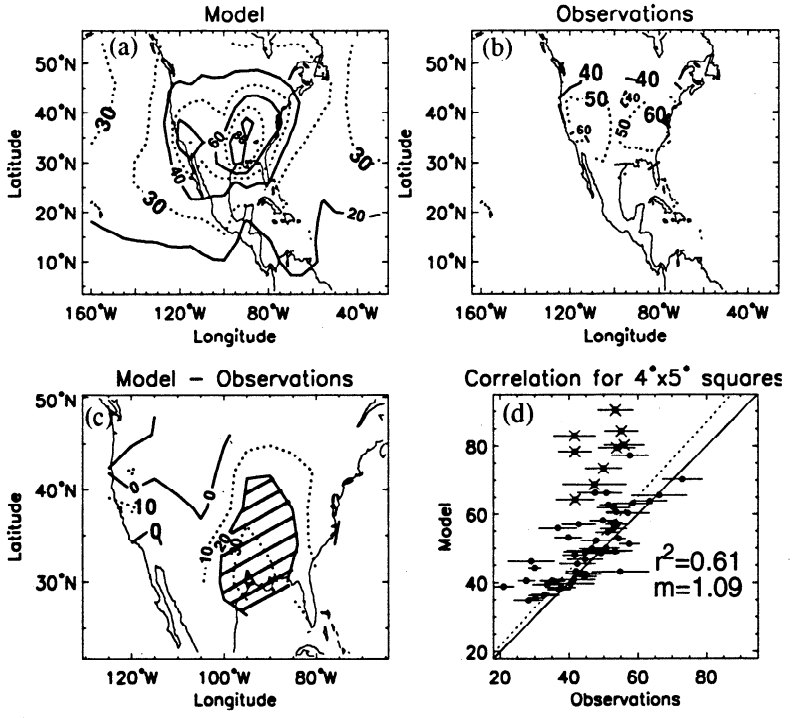

Figure 3. Median summertime (June-August) ozone concentrations (in ppbv) at 1300–1600 local time (a) simulated by the model in rural surface air (including representative sampling of aged pollution plumes), and (b) measured at the EPA/AIRS network of surface sites [*Fiore et al.*, 1997]. (c) Difference between model and observations (in ppbv); the area of the south central United States where ozone is overestimated by more than 20 ppbv is shaded. (d) Comparison of simulated and observed median concentrations (in ppbv) in individual 4°×5° grid squares. In Figure 3d, horizontal bars represent interannual variability of the observations in the 1980–1995 record (±1 standard deviation); the solid line is the 1:1 line, and the dashed line is a linear regression calculated excluding points in the south central U.S. (marked with crosses, corresponding to the shaded region in Figure 3c).

ΔX of these correlations (where X is CO or NO_y-NO_x) provide a measure of the ozone production efficiency that is relatively insensitive to variations in transport [*Parrish et al.*, 1993b; *Trainer et al.*, 1993; *Chin et al.*, 1994]. Table 5 compares simulated and observed slopes at representative sites.

Summertime values of $\Delta O_3/\Delta CO$ in the model for eastern North America are typically in the range 0.25–0.33, consistent with observations [*Chin et al.*, 1994]. One exception is Kinterbish, Alabama, where the model slope of 0.60 considerably exceeds the observed value of 0.32 [*Chin et al.*, 1994]. This is likely a symptom of the problems discussed earlier regarding the model overestimate of ozone in the south central United States.

Simulated slopes for $\Delta O_3/\Delta(NO_y\text{-}NO_x)$ at sites in eastern North America are typically in the range 6–10, with high values occurring in the southeast United States and lower values in the northeast United States, as found in the observations [*Trainer et al.*, 1993; *Olszyna et al.*, 1994]. However, the slopes in the model are consistently lower than observed values by about 20%. Background ozone concentrations, as indicated by the intercept of the regression line (b), are close to observed values. An explanation for the low $\Delta O_3/\Delta(NO_y\text{-}NO_x)$ slope in the model is the tendency of the model to overestimate HNO_3 concentrations in surface air, as discussed above.

4.6. Sensitivity To Chemical Assumptions

We conducted a number of sensitivity studies to examine the effects of various chemical assumptions made in the model (section 3). When the model does not include deposition of hydroxy organic nitrates from isoprene (ISN2), the surface concentration of ozone increases by about 3 ppbv throughout the eastern United States, largely as a result of increased recycling of ISN2 to NO_x. The concentrations of NO_x, PAN, and HNO_3 over the eastern United States increase by about 5–10%. Concentrations of CO increase slightly as a result of increased production from ISN2 oxidation. Similarly, CH_2O concentrations increase by about 5%.

When the model does not include the aerosol sink for HO_2, concentrations of H_2O_2 increase by 25–100% over the eastern United States, and ozone concentrations increase by up to 3 ppbv. The concentrations of OH increase, causing more rapid oxidation of NO_x to HNO_3 and thus a decrease of NO_x concentrations (by up to 10–15% in the northeast United States). Concentrations of PAN increase by up to 15% in the northeastern United States as a result of the more rapid oxidation of NMHCs. The concentrations of CH_2O decline by up to 10%, most likely as a result of increased production and deposition of organic hydroxyperoxides. Additionally, there is a small decline in CO concentrations.

If an aerosol loss reaction for organic RO_2 radicals is added to the model (with γ=0.1), ozone in surface air decreases by up to 4 ppbv throughout the eastern United States. The concentration of NO_x decreases by up to 10% in the southeastern United States as a result of the loss to aerosols of nitrogen-containing peroxy radicals. Concentrations of PAN decrease by 10–15% throughout the eastern United States. In the northeastern United States, NO_x increases by about 10% as a result of decreased conversion to

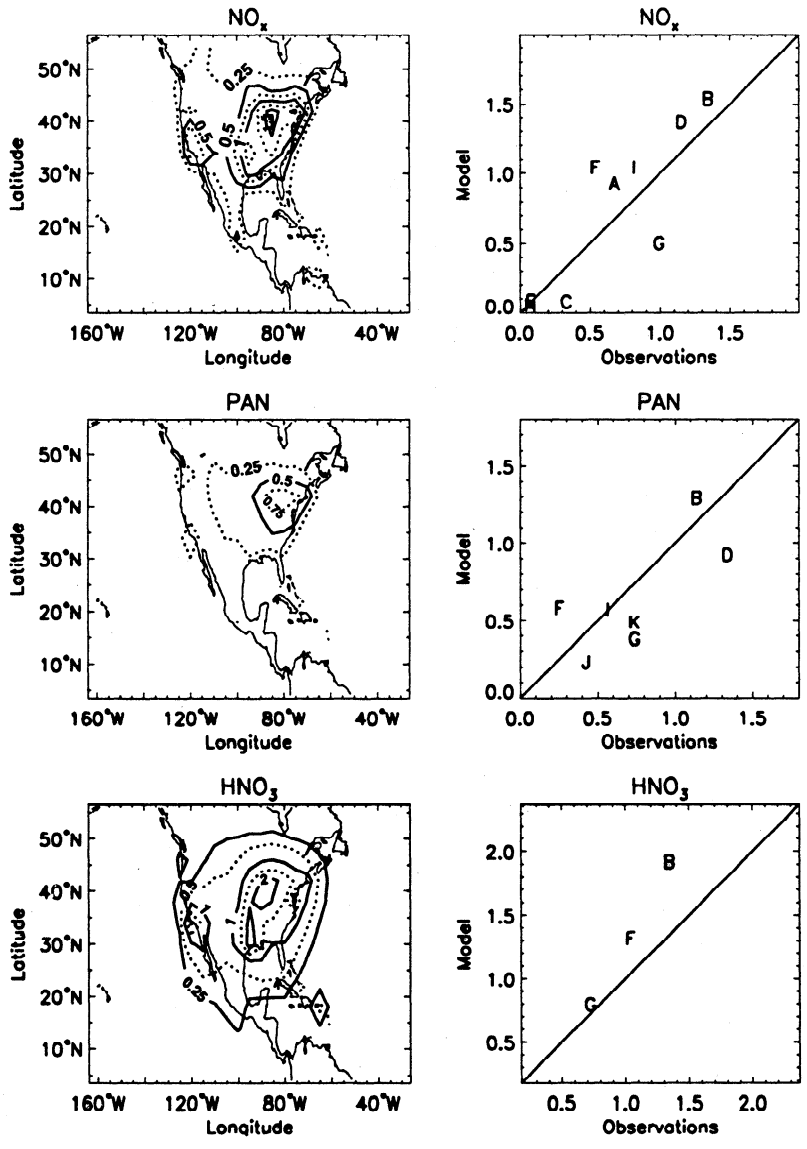

Figure 4. (left) Mean summertime concentrations (in ppbv) of reactive nitrogen species simulated by the model in rural surface air at 1300–1600 local time. (right) Comparison of simulated and observed concentrations (in ppbv) for the sites and statistics listed in Table 3.

Table 4. Partitioning of Summertime NO_y Concentrations at Nonurban Sites

	NO_x/NO_y		PAN/NO_y		$(HNO_3(g)+NO_3^-)/NO_y$ [a]	
	Model	Obs.	Model	Obs.	Model	Obs.
Scotia, Pennsylvania	28	27	17	21	32	31
Egbert, Ontario	23	39	16	20	35	35
Bondville, Illinois[b]	28	27	14	13	39	---
Harvard Forest, Massachusetts	27	25	20	---	34	---

Simulated and observed (obs.) median afternoon ratios (1300–1600 LT) for the summer months (June–August). Observations at Scotia, Egbert, and Bondville [*Parrish et al.*, 1993a] are for 1988; those at Harvard Forest [*Munger et al.*, 1996] are for 1990-1995. Partitioning is in percent.

[a]The model does not distinguish between HNO_3 (g) and NO_3^- aerosol.

[b]The HNO_3/NO_y ratio at Bondville, Illinois is excluded from our comparisons since the nitric acid measurements there were averages over 12-hour periods and lacked diurnal resolution.

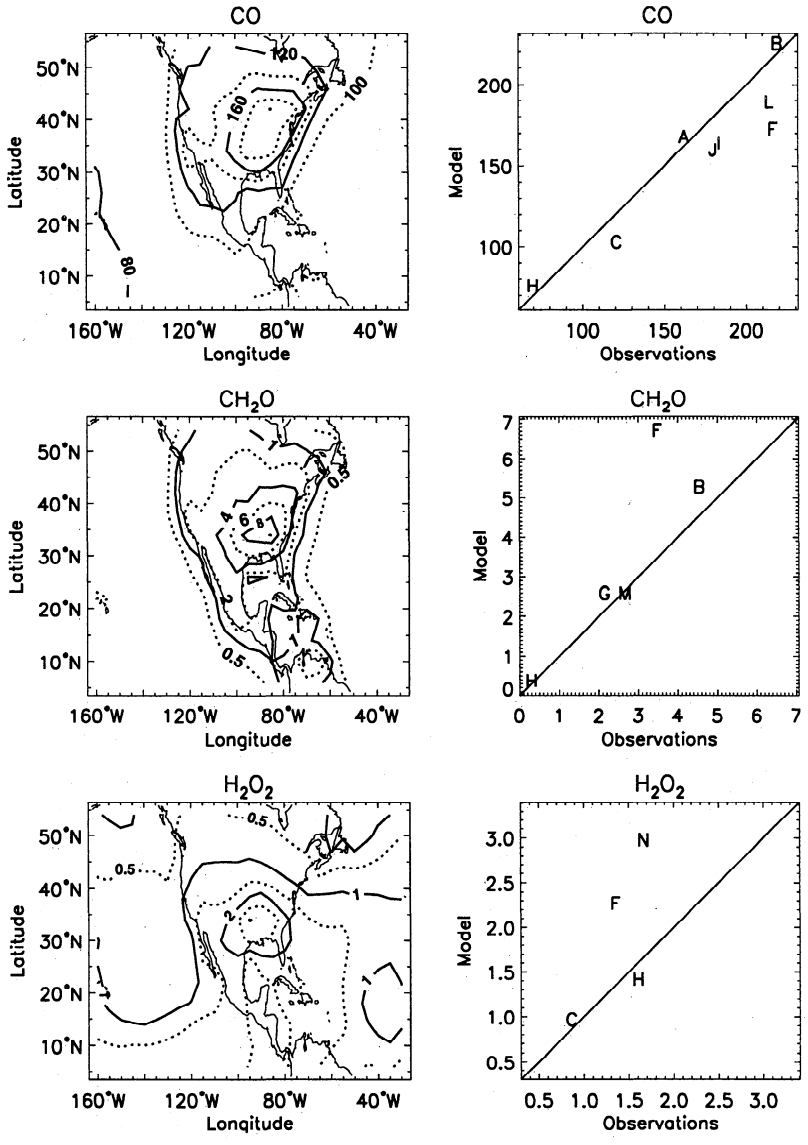

Figure 5. (left) Mean summertime concentrations (in ppbv) of CO, CH_2O, and H_2O_2 simulated by the model in rural surface air at 1300–1600 local time. (right) Comparison of simulated and observed concentrations (in ppbv) for the sites and statistics listed in Table 3.

PAN and slower oxidation by OH, the concentration of which decreases by a few percent.

5. Export of NO_x Pollution From the United States

5.1. Budgets of NO_y Species in the U.S. Boundary Layer

A model budget for NO_y species in the U.S. boundary layer is presented in Table 6. We define the U.S. boundary layer as the atmospheric domain extending horizontally over the delineated area in Figure 1 and vertically from the surface to 2.6 km altitude (top of model layer 3). The emission rate of NO_x within the domain is 1.34 Gmol d^{-1}. Import of NO_y emitted outside the region, or advected from the boundaries of the model domain, is negligibly small. The short lifetime of NO_x allows most of it to be oxidized to other species within the continental boundary layer. Net transport of NO_x out of the region is only 9% of the total emitted and takes place primarily by wet convection over the eastern United States [*Jacob et al.*, 1993a; *Liang et al.*, this issue]. About 53% of the NO_x emitted is converted to nitric acid within the U.S. boundary layer. Smaller amounts are converted to PANs, ISN2, and organic nitroxyperoxides (net production rates of 8, 16, and 6% of NO_x emissions, respectively). Dry deposition of NO_2 amounts to 5.5% of NO_x emissions.

Most of the nitric acid produced in the U.S. boundary layer is lost within the region by either dry or wet deposition (24 and 22% of NO_x emissions, respectively). There is a horizontal flux of HNO_3 out of the region (equal to 7% of NO_x emissions), while there is a vertical flux into the region (1% of NO_x emissions). This downward flux of HNO_3 is attributable to production in the middle troposphere of nitric acid from NO_x transported up from the surface, followed by descent into the boundary layer. The net chemical production of PANs in the region is balanced primarily by export from the region, representing 5% of the NO_x emissions. Loss of PANs by dry deposition is smaller, equal to 3% of NO_x emissions. The export flux of the organic hydroxynitrate species

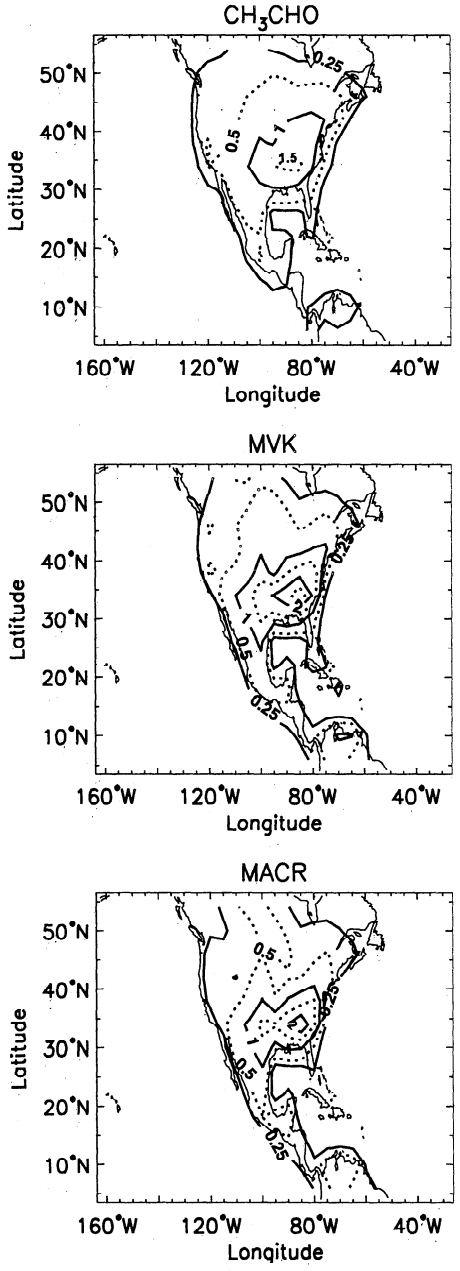

Figure 6. Mean summertime rural concentrations (in ppbv) of acetaldehyde, methyl vinyl ketone, and methacrolein simulated by the model in rural surface air at 1300–1600 local time.

ISN2 is only 1% of NO_x emissions as a result of its rapid removal by dry and wet deposition. In our model, the organic peroxides are not transported, so the net production of nitrogen-containing peroxides (6% of NO_x emissions) is balanced only by deposition.

The net export flux of NO_y from the summertime U.S. boundary layer in our model is 22% of NO_x emissions (0.30 Gmol d^{-1}). This is roughly consistent with the estimate by *Kasibhatla et al.* [1993] that 25–30% of NO_x emissions in the United States are exported out of the continental boundary layer as NO_y on an annual basis. In order to estimate the potential source of NO_x in the remote troposphere resulting from this export, we exclude the contribution from HNO_3, which we expect to be removed eventually by deposition (rather than recycled back to NO_x). The remaining export flux, that of NO_x plus organic nitrates, is 16% of NO_x emissions (0.22 Gmol d^{-1}).

This potential source of NO_x to the remote troposphere can be compared to estimates for other sources of NO_x in the northern hemisphere during summertime [*Wang et al.*, 1997a], including lightning (0.63 Gmol d^{-1}), the stratosphere (0.01 Gmol d^{-1}), and aircraft emissions (0.09 Gmol d^{-1}). The United States contributes approximately 35% of the total fossil fuel combustion NO_x in the Northern Hemisphere [*Dignon*, 1992]. We expect therefore that export of pollution NO_x from the industrial continents makes a large contribution to NO_x levels in the NH troposphere in summer, comparable to the source from lightning. *Lamarque et al.* [1996] came to a similar conclusion, finding that at 900 mbar during summertime, fossil fuel emissions accounted for approximately 50% of the NO_x on a zonal mean basis at 30°–90°N, with lightning contributing about 30%.

Of the total export flux of NO_x plus organic nitrates from the U.S. boundary layer, almost half (0.10 Gmol d^{-1}) is in the form of organic nitrates. PAN accounts for about half of the exported organic nitrates, with the balance composed of other peroxyacyl nitrates, isoprene nitrates, and alkyl nitrates (Table 6). The important role of PAN in the export of NO_y from source regions in our model has also been found in previous model studies [*Kasibhatla et al.*, 1993; *Moxim et al.*, 1996]. In our model, however, we also find an important contribution from other organic nitrates which were not included in previous models.

5.2. Influence on the Upper Troposphere

Deep convection over the United States injects NO_x from fossil fuel combustion into the upper troposphere, adding to the NO_x sources in that region from lightning, aircraft, and downward transport from the stratosphere. We can define the convective injection in our model by the upward flux at 400 mbar (top of model layer 5) over the United States domain defined in Figure 1. The upward flux of NO_y consists mainly of NO_x and PAN (0.04 and 0.02 Gmol d^{-1}, respectively). Upward transport of HNO_3 is suppressed by the efficient scavenging of HNO_3 in wet convective updrafts. There is a small downward flux of HNO_3 (0.01 Gmol d^{-1}) and small upward fluxes of PMN, PPN, and R4N2 (adding up to 0.01 Gmol d^{-1}). The net upward transport of NO_y into the upper troposphere above the United States is equal to 0.07 Gmol d^{-1} (5% of NO_x emissions). This flux has a maximum above the eastern United States, where NO_x emissions are highest, and a secondary maximum above the central United States, where there is strong deep vertical convection. Recent aircraft observations over the central United States in spring show a dominant source of NO_x at 8–12 km altitude from convective injection of pollution [*Jaeglé et al.*, 1997].

Zonal mean estimates for other sources of NO_x to the upper troposphere in the latitude range of the United States (24°–48°N) are 0.09 Gmol d^{-1} from lightning, 0.01 Gmol d^{-1} from the stratosphere, and 0.03 Gmol d^{-1} from aircraft [*Baughcum et al.*, 1996; *Wang et al.*, 1997a]. Thus, the major sources of NO_x in the midlatitude upper troposphere, based on our model results, are lightning and convective injection of pollution. The sources from aircraft and the stratosphere are smaller. Our finding that convective injection of anthropogenic NO_x makes a large contribution to the budget of NO_x in the upper troposphere at northern midlatitudes agrees with the previous model studies of *Ehhalt et al.* [1992] and *Brasseur et al.* [1996b], but it is at odds with the study of *Kasibhatla* [1993] who argued that aircraft and transport from the stratosphere should dominate, and that of *Lamarque et al.* [1996] who found that lightning and aircraft should be the most important sources. *Ehhalt et al.* [1992] found that 2% of surface NO_x emis-

Table 5. O_3:CO and O_3:(NO_y-NO_x) Correlations at Nonurban Sites

Site	Location	Period	X	$\frac{\Delta O_3}{\Delta X}$	r^2	b (ppbv)	Obs./ Model	Reference
Scotia, Pennsylvania	41°N, 78°W	July-Aug., 1988	CO	0.28	0.43	--	obs.	*Chin et al.* [1994]
				0.29	0.79	--	model	
		July-Aug., 1988	NO_y-NO_x	8.5	0.99[a]	35	obs.	*Trainer et al.* [1993]
				6.9	0.87	36	model	
Metter, Georgia	33°N, 82°W	July-Aug., 1991	NO_y-NO_x	11.4	0.78	34	obs.	*Kleinman et al.* [1994]
				9.2	0.84	34	model	
Harvard Forest, Massachusetts	42°N, 72°W	June-Aug., 1990-1992	CO	0.28	0.78	--	obs.	*Chin et al.* [1994]
				0.26	0.75	--	model	

Observations and model results are for 1300–1600 local time in June–August. Periods for which $NO_x/NO_y \geq 0.3$ mol/mol are excluded from the O_3:CO correlations, as they are indicative of fresh pollution where ozone production has not yet been realized [*Chin et al.*, 1994]. We report the slope ($\Delta O_3/\Delta X$) and intercept b (in ppbv O_3, for X=NO_y-NO_x) of the least squares linear regressions and the correlation coefficients r^2.

[a]The data are binned, explaining the high r^2 value.

sions at northern mid-latitudes reach the upper troposphere, somewhat lower than the 4.5% value reported here (or 3% if we do not include the contributions from NO_y species other than NO_x).

6. Sensitivity Studies

The organic nitrates PAN, PMN, and ISN2 make important contributions to the export of NO_y from the U.S. boundary layer in our model (Table 6). Oxidation of isoprene is responsible for most of PAN formation and for all of PMN and ISN2 formation. Omitting isoprene emissions in the model has a major effect on the budgets of NO_y species (Figure 7). Concentrations of ozone (Figure 8) decrease considerably over the eastern United States, in some places by more than 25 ppbv. The concentration of PAN (Figure 9) is reduced by 40–60% throughout most of the domain. The absence of isoprene causes OH concentrations to increase by a factor of 2 or more throughout the United States, facilitating oxidation of NO_x to HNO_3, which further decreases PAN formation. More rapid oxidation of NO_x to HNO_3 causes concentrations of NO_x to be reduced over the southeast United States (Figure 9) and nitric acid to increase by 50-150%.

In the absence of isoprene, the net export of PANs out of the U.S. boundary layer decreases from 0.07 Gmol d^{-1} to only 0.01 Gmol d^{-1}. Export of alkyl nitrates remains approximately unchanged, while export of ISN2 is reduced to zero (Figure 7). As a result of decreased conversion to organic nitrates, the amount of NO_x that is exported increases from 0.12 to 0.14 Gmol d^{-1}. The increase in nitric acid results in increased deposition and net export of this species (0.92 and 0.12 Gmol d^{-1}, respectively). Overall, the net export of NO_x and organic nitrates from the U.S. continental boundary layer to the global atmosphere is decreased by about 22% when isoprene emissions are omitted.

When the model is run with anthropogenic emissions of NMHCs omitted, the effect on the NO_y budget over the United States is small. The largest effects occur near southern California and in the northeast United States, where anthropogenic NMHC

Table 6. Summertime Budget for NO_y Species in U.S. Boundary Layer

Species	Emission	Chemical (P-L)[a]	Dry Deposition	Wet Deposition	Net Export
NO_x	1.34	-1.14	0.07	---	0.12
PAN	---	0.08	0.03	---	0.05
HNO_3	---	0.71	0.32	0.30	0.08
PMN	---	0.02	0.01	---	0.02
PPN	---	0.01	0.00	---	0.01
ISN2	---	0.21	0.11	0.08	0.02
R4N2	---	0.02	0.00	---	0.01
Organic nitroxyperoxides[b]	---	0.08	0.08	---	---

Mean model values for June–August. We define the U.S. boundary layer (see Figure 1) as the region extending from 67.5°–127.5°W and 24°–48°N, and from the surface to approximately 2.6 km altitude (top of model layer 3). Summertime budget terms are in Gmol d^{-1}.

[a]Chemical production minus loss, including kinetic reactions and photolysis, but excluding emission and deposition.

[b]Not a transported tracer in our model.

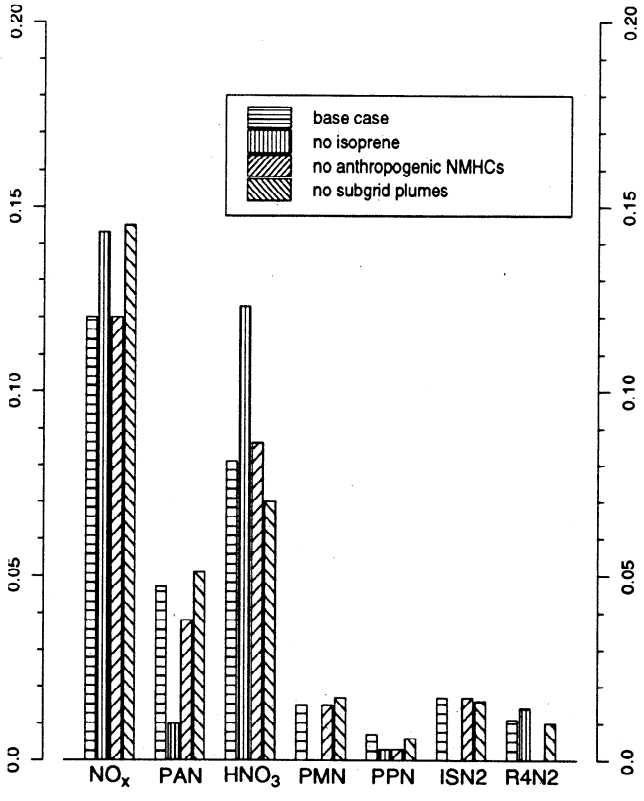

Figure 7. Mean summertime export fluxes (Gmol d^{-1}) of reactive nitrogen species from the U.S. boundary layer defined in Figure 1. See text (section 6) for descriptions of the emission scenarios.

emissions are highest. There are small (~2%) decreases in surface concentrations of O_3 (Figure 8) and NO_x (Figure 9) throughout the United States, with larger (~5%) decreases over southern California. Concentrations of PAN (Figure 9) decrease by 5–20% throughout the United States, while HNO_3 increases by about 5%. In southern California, the changes in PAN and HNO_3 are larger, approximately -50% and +15%, respectively. There is a considerable decrease in PPN (typically 25–60%) and R4N2 (~90%), both of which were fairly minor components of NO_y in the standard simulation. Concentrations of OH are increased by a small amount, with a maximum effect of 10–25% occurring in the Northeast and in southern California. As shown in Figure 7, the export flux of NO_x plus organic nitrates from the U.S. boundary layer is reduced by 11% when anthropogenic NMHCs are omitted, as compared to 22% when isoprene is omitted. Export of PANs is reduced by 19% when anthropogenic NMHCs are omitted, compared to 81% when isoprene is omitted.

The nonlinear dependence of NO_x budgets for the United States on NO_x emissions was investigated using sensitivity simulations in which NO_x emission fluxes were increased or decreased uniformly by 25%. Increasing NO_x emissions by 25% causes OH concentrations to increase by about 20% over most of the United States due to higher concentrations of both NO_x and ozone. As a result, the conversion of NO_x to HNO_3 is facilitated. Net production of nitric acid within the U.S. boundary layer is enhanced from 53% of NO_x emissions in the standard simulation to 58% of NO_x emissions in the simulation with higher NO_x. The total export of organic nitrates from the U.S. boundary layer decreases from 7.2% of NO_x emissions to 6.6%. The decreased importance of organic nitrates when NO_x emissions are increased is consistent with the previous results of *Atherton and Penner* [1990], who found that the contribution of organic nitrates to NO_y increased in model simulations with higher hydrocarbon-to-NO_x ratios. We find that the total export of NO_x plus organic nitrates out of the U.S. boundary layer decreases from 16.2 to 15.2% of NO_x emissions when these emissions are increased by 25%. Reverse effects of similar magnitude are found in the simulation with reduced NO_x emissions.

About half of total NO_x emissions in the United States in the model are released in subgrid urban and power plant plumes, where they age for 8 hours before being diluted to the grid scale. A shortcoming in the subgrid treatment of pollution plumes in the model is that it does not allow for cross-gridbox transport of the plumes. We conducted a sensitivity simulation without subgrid plumes, that is, with NO_x injected directly into the 4°×5° grid box. The more rapid dispersal of NO_x results in greater production of ozone, leading to an increase in the surface concentration of ozone by over 5 ppbv throughout most of the eastern United States, and up to 15 ppbv in the southeast. The more rapid dispersal of NO_x into the rural boxes increases the chemical lifetime of NO_x, since the OH concentrations are lower in the rural boxes than in the pollution plumes. The increased chemical lifetime, along with the elimination of the transport restrictions imposed on the subgrid plumes, allows more of the NO_x to be exported from the U.S. boundary layer. The total export of NO_x plus organic nitrates increases from 0.22 to 0.25 Gmol d^{-1}, now representing 18.4% of the NO_x emissions.

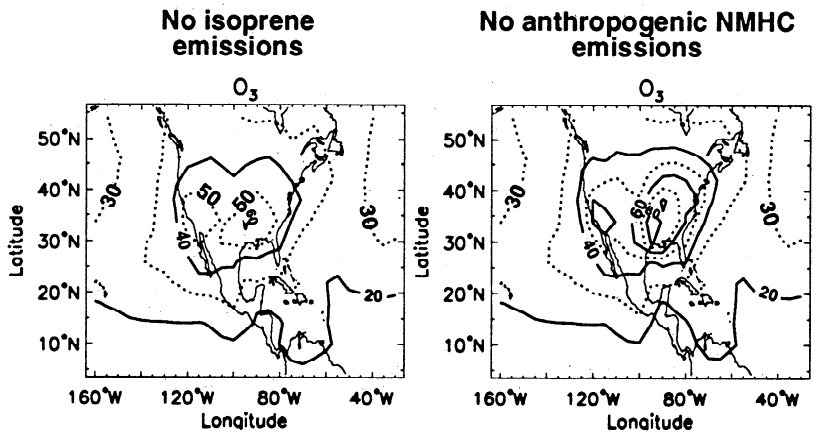

Figure 8. Median summertime ozone concentrations (in ppbv) in rural surface air at 1300–1600 local time, for the model with (left) no isoprene emissions or (right) no anthropogenic NMHC emissions.

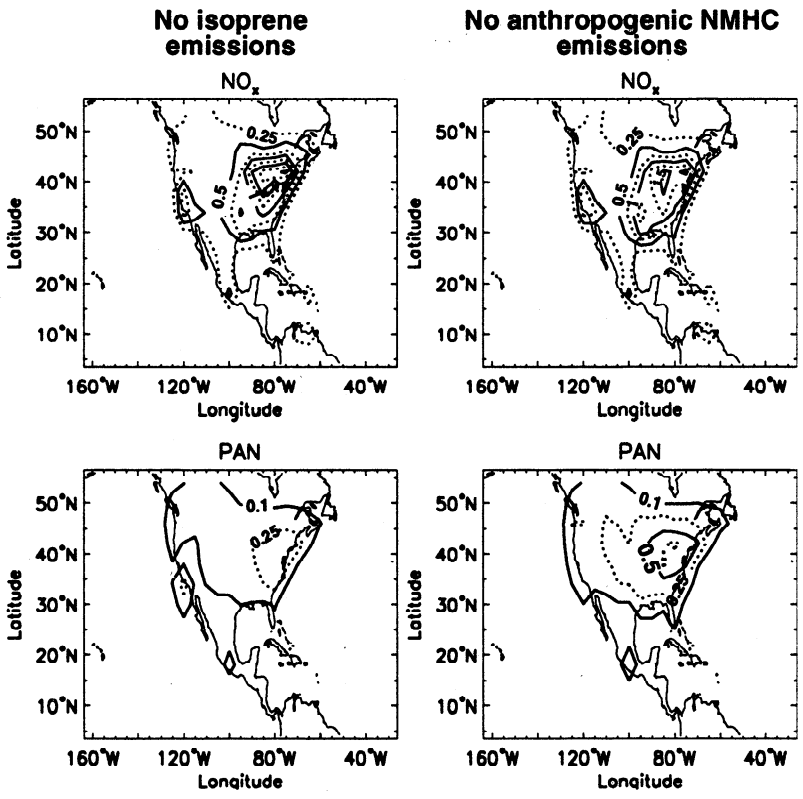

Figure 9. Mean summertime concentrations of NO_x and PAN (in ppbv) in rural surface air at 1300–1600 local time, for the model with (left) no isoprene emissions or (right) no anthropogenic NMHC emissions.

7. Conclusions

We have performed a simulation of summertime photochemistry over North America using a continental-scale three-dimensional model, with a chemical mechanism that includes detailed treatment for anthropogenic and biogenic hydrocarbons and their oxidation products. The model produces a reasonable simulation of observed concentrations of O_3 and its precursors in surface air over the United States. The most significant discrepancy is the overestimate of ozone by more than 20 ppbv in the south central United States. We attribute this overestimate primarily to the northeastward displacement of the Bermuda High in the GISS GCM. The model generally reproduces the observed median concentrations of the reactive nitrogen species NO_x, PAN, and HNO_3 to within 30%, as well as the partitioning among these species to within 20%. Concentrations of CH_2O are simulated to within 10% at the few sites where seasonal observations are available. Predicted concentrations of H_2O_2 are too high. The observed relationships of ozone with CO and with NO_y-NO_x are reproduced closely by the model.

We find our model results to be sensitive to certain key assumptions about the chemistry. Our standard mechanism includes rapid wet and dry deposition of the hydroxy organic nitrates derived from isoprene (ISN2), and a rapid aerosol loss reaction for HO_2 radicals in which reaction products are assumed inert. Sensitivity tests indicate that if deposition of ISN2 is excluded from our model, mean concentrations of O_3, NO_x and PAN increase by 5–10% over the eastern United States. If the model is run without the aerosol sink for HO_2, predicted surface concentrations of H_2O_2 increase by 25–100%, while concentrations of O_3 increase by up to 3 ppbv, and those of NO_x increase by up to 15%. If an aerosol loss reaction for organic RO_2 radicals is added to the model, concentrations of ozone in surface air decrease by up to 4 ppbv, and those of PAN decrease by 10-15%; the concentration of NO_x decreases by up to 10% in the southeast United States and increases by about 10% in the northeast United States.

We find that 9% of the NO_x emitted in the United States is exported as NO_x from the continental boundary layer to the global atmosphere; 3.5% is exported as PAN, and 3.7% is exported as other organic nitrates. This indicates the important role played by NMHCs in determining the amount of NO_x from polluted continents that is made available to the global atmosphere. The total export of NO_x plus organic nitrates from the U.S. continental boundary layer, equal to 0.22 Gmol d^{-1}, provides a larger source of NO_x in the northern hemisphere troposphere than sources from aircraft or cross-tropopause transport; it is about a factor of 3 smaller than the hemispheric source from lightning. Deep convection from the U.S. boundary layer is estimated to contribute 0.06 Gmol d^{-1} of NO_x to the upper troposphere at northern midlatitudes (400–150 mbar, 24°–48°N). This is considerably larger than the zonal mean source of NO_x from aircraft in that same latitude and altitude band and is about half as large as the source from lightning.

Isoprene is the most important hydrocarbon modifying the export of NO_y species from the U.S. boundary layer. When isoprene is omitted from the model, the concentrations and export fluxes of organic nitrates decrease by 70-80%, while the export of NO_x increases by about 20%. The overall export of NO_x plus organic nitrates from the U.S. boundary layer is reduced by about 20%. Anthropogenic NMHC emissions have less of an effect. The role of isoprene in promoting the export of PANs has important

implications for NO_x in the remote troposphere, where decomposition of PAN provides a major source of NO_x [*Fan et al.*, 1994; *Singh et al.*, 1994b]. Our conclusions about the importance of isoprene are based on present estimates for the emission rate of isoprene, and a large uncertainty remains attached to these estimates. If the isoprene emission rate in our model were reduced by a factor of 2, we find that the impacts of isoprene and anthropogenic NMHCs on the export of NO_x plus organic nitrates from the U.S. boundary layer would be comparable, although production and export of PANs would still be driven primarily by isoprene. We conclude that, in the context of global-scale three-dimensional models, proper representation of the export of NO_x emissions out of polluted continental boundary layers requires inclusion of the chemistry of NMHCs, particularly isoprene.

Acknowledgments. We thank our colleagues J.W. Munger, for providing us with unpublished data from Harvard Forest, J.A. Logan, for compiling several of the emissions inventories we have used, and A.M. Fiore, for her analysis of the EPA/AIRS ozone data. This work was supported by the National Oceanic and Atmospheric Administration (NA46GP0138), the National Science Foundation (NSF-ATM-96-12282), and the National Aeronautics and Space Administration (NASA-NAGW-2632 and NASA-NAG5-2688). L.W. Horowitz received support from the National Aeronautics and Space Administration Graduate Student Fellowship in Global Change.

References

Aschmann, S.M., and R. Atkinson, Formation yields of methyl vinyl ketone and methacrolein from the gas-phase reaction of O_3 with isoprene, *Environ. Sci. Technol.*, *28*, 1539-1542, 1994.

Atherton, C.S., and J.E. Penner, The effects of biogenic hydrocarbons on the transformation of nitrogen oxides in the troposphere, *J. Geophys. Res.*, *95*, 14,027-14,038, 1990.

Atkinson, R., Gas-phase tropospheric chemistry of organic compounds: A review, *Atmos. Environ., Part A*, *24*, 1-41, 1990.

Atkinson, R., Gas-phase tropospheric chemistry of organic compounds, *J. Phys. Chem. Ref. Data Monogr.*, *2*, 1-216, 1994.

Atkinson, R., D.L. Baulch, R.A. Cox, R.F. Hampson Jr., J.A. Kerr, and J. Troe, Evaluated kinetic and photochemical data for atmospheric chemistry, *J. Phys. Chem. Ref. Data*, *21*, 1125-1568, 1992.

Atlas, E.L., and B.A. Ridley, The Mauna Loa Observatory Photochemistry Experiment: Introduction, *J. Geophys. Res.*, *101*, 14,531-14,541, 1996.

Bakwin, P.S., et al., Reactive nitrogen oxides and ozone above a taiga woodland, *J. Geophys. Res.*, *99*, 1927-1936, 1994.

Balkanski, Y.J., Atmospheric residence times of continental aerosols, Ph.D. dissertation, Harvard Univ., Cambridge, Mass., 1991.

Balkanski, Y.J., D.J. Jacob, G.M. Gardner, W.C. Graustein, and K.K. Turekian, Transport and residence times of tropospheric aerosols inferred from a global three-dimensional simulation of ^{210}Pb, *J. Geophys. Res.*, *98*, 20,573-20,586, 1993.

Baughcum, S.L., T.G. Tritz, S.C. Henderson, and D.C. Pickett, Scheduled civil aircraft emission inventories for 1992: Database development and analysis, *NASA Rep. CR-4700*, 1996.

Benkovitz, C.M., M.T. Scholtz, J. Pacyna, L. Tarrasón, J. Dignon, E.C. Voldner, P.A. Spiro, J.A. Logan, and T.E. Graedel, Global gridded inventories of anthropogenic emissions of sulfur and nitrogen, *J. Geophys. Res.*, *101*, 29,239-29,253, 1996.

Brasseur, G.P., D.A. Hauglustaine, and S. Walters, Chemical compounds in the remote Pacific troposphere: Comparison between MLOPEX measurements and chemical transport model calculations, *J. Geophys. Res.*, *101*, 14,795-14,813, 1996a.

Brasseur, G.P., J.-F. Müller, and C. Granier, Atmospheric impact of NO_y emissions by subsonic aircraft: A three-dimensional model study, *J. Geophys. Res.*, *101*, 1423-1428, 1996b.

Cantrell, C.A., et al., Peroxy radicals as measured in ROSE and estimated from photostationary state deviations, *J. Geophys. Res.*, *98*, 18,355-18,366, 1993.

Cantrell, C.A., R.E. Shetter, T.M. Gilpin, J.G. Calvert, F.L. Eisele, and D.J. Tanner, Peroxy radical concentrations measured and calculated from trace gas measurements in the Mauna Loa Observatory Photochemistry Experiment 2, *J. Geophys. Res.*, *101*, 14,653-14,664, 1996.

Carter, W.P.L., A detailed mechanism for the gas-phase atmospheric reactions of organic compounds, *Atmos. Environ., Part A*, *24*, 481-518, 1990.

Carter, W.P.L., and R. Atkinson, Development and evaluation of a detailed mechanism for the atmospheric reactions of isoprene and NO_x, *Int. J. Chem. Kinet.*, *28*, 497-530, 1996.

Chameides, W.L., R.W. Lindsay, J. Richardson, and C.S. Kiang, The role of biogeninc hydrocarbons in urban photochemical smog: Atlanta as a case study, *Science*, *241*, 1473-1475, 1988.

Chameides, W.L., et al., Ozone precursor relationships in the ambient atmosphere, *J. Geophys. Res.*, *97*, 6037-6055, 1992.

Chin, M., and D.J. Jacob, Anthropogenic and natural contributions to tropospheric sulfate: A global model analysis, *J. Geophys. Res.*, *101*, 18,691-18,699, 1996.

Chin, M., D.J. Jacob, J.W. Munger, D.D. Parrish, and B.G. Doddridge, Relationship of ozone and carbon monoxide over North America, *J. Geophys. Res.*, *99*, 14,565-14,573, 1994.

Chin, M., D.J. Jacob, G.M. Gardner, M.S. Foreman-Fowler, P.A. Spiro, and D.L. Savoie, A global three-dimensional model of tropospheric sulfate, *J. Geophys. Res.*, *101*, 18,667-18,690, 1996.

Crutzen, P.J., The role of NO and NO_2 in the chemistry of the troposphere and stratosphere, *Ann. Rev. Earth Planet. Sci.*, *7*, 443-472, 1979.

DeMore, W.B., S.P. Sander, D.M. Golden, R.F. Hampson, M.J., Kurylo, C.J. Howard, A.R. Ravishankara, C.E. Kolb, and M.J. Molina, Chemical kinetics and photochemical data for use in stratospheric modeling, *JPL Publ.*, *94-26*, 1994.

Dignon, J., NO_x and SO_x emissions from fossil fuels: A global distribution, *Atmos. Environ., Part A*, *26*, 1157-1163, 1992.

Ehhalt, D.H., F. Rohrer, and A. Wahner, Sources and distribution of NO_x in the upper troposphere at northern midlatitudes, *J. Geophys. Res.*, *97*, 3725-3738, 1992.

Environment Canada, Estimation of the effects of various municipal waste management strategies on greenhouse gas emissions, summary report, Ottawa, Ontario, 1995.

Environmental Protection Agency (EPA), The 1985 NAPAP emissions inventory (version 2): Development of the annual data and modeler's tapes, *EPA-600/7-89-012a*, Research Triangle Park, N. C., 1989.

Environmental Protection Agency (EPA), National air quality and emissions trends report, 1992, *EPA-454/R-93-031*, Research Triangle Park, N. C., 1993.

Environmental Protection Agency (EPA), National air pollutant emission trends, 1900-1994, *EPA-454/R-95-011*, Research Triangle Park, N. C., 1995.

Fan, S.-M., D.J. Jacob, D.L. Mauzerall, J.D. Bradshaw, S.T. Sandholm, D.R. Blake, H.B. Singh, R.W. Talbot, G.L. Gregory, and G.W. Sachse, Origin of tropospheric NO_x over subarctic eastern Canada in summer, *J. Geophys. Res.*, *99*, 16,867-16,877, 1994.

Fehsenfeld, F., et al., Emissions of volatile organic compounds from vegetation and the implications for atmospheric chemistry, *Global Biogeochem. Cycles*, *6*, 389-430, 1992.

Fiore, A.M., J.H. Yin, D.J. Jacob, and J.A. Logan, Long-term trends in ground level ozone over the contiguous United States, 1980-1995, *J. Geophys. Res.*, in press, 1997.

Goldstein, A.H., S.C. Wofsy, and C.M. Spivakovsky, Seasonal variations of nonmethane hydrocarbons in rural New England: Constraints on OH concentrations in northern midlatitudes, *J. Geophys. Res.*, *100*, 21,023-21,033, 1995.

Goldstein, A.H., S.-M. Fan, M.L. Goulden, J.W. Munger, and S.C. Wofsy, Emissions of ethene, propene, and 1-butene by a midlatitude forest, *J. Geophys. Res.*, *101*, 9149-9157, 1996.

Graedel, T.E., M.L. Mandich, and C.J. Weschler, Kinetic model studies of atmospheric droplet chemistry, 2, Homogeneous transition metal chemistry in raindrops, *J. Geophys. Res.*, *91*, 5205-5221, 1986.

Grosjean, D., E. Grosjean, and E.L. Williams II, The reaction of ozone with MPAN, $CH_2=C(CH_3)C(O)OONO_2$, *Environ. Sci. Technol.*, *27*, 2548-2552, 1993a.

Grosjean, D., E.L. Williams II, and E. Grosjean, Gas phase reaction of the hydroxyl radical with the unsaturated peroxyacyl nitrate $CH_2=C(CH_3)C(O)OONO_2$, *Int. J. Chem. Kinet.*, *25*, 921-929, 1993b.

Grosjean, D., E.L. Williams II, and E. Grosjean, Atmospheric chemistry of isoprene and of its carbonyl products, *Environ. Sci. Technol.*, *27*, 830-840, 1993c.

Guenther, A., et al., A global model of natural volatile organic carbon emissions, *J. Geophys. Res.*, *100*, 8873-8892, 1995.

Hansen, J., G. Russell, D. Rind, P. Stone, A. Lacis, S. Lebedeff, R. Ruedy, and L. Travis, Efficient three-dimensional global models for climate studies: Models I and II, *Mon. Weather Rev.*, *111*, 609-662, 1983.

Hansen, J., M. Sato, and R. Ruedy, Radiative forcing and climate response, *J. Geophys. Res.*, *102*, 6831-6864, 1997.

Hanson, D.R., J.B. Burkholder, C.J. Howard, and A.R. Ravishankara, Measurement of OH and HO_2 radical uptake coefficients on water and sulfuric acid surfaces, *J. Phys. Chem.*, *96*, 4979-4985, 1992.

Hartsell, B.E., V.P. Aneja, and W.A. Lonneman, Relationships between peroxyacetyl nitrate, O_3, and NO_y at the rural Southern Oxidants Study site in central Piedmont, North Carolina, site SONIA, *J. Geophys. Res.*, *99*, 21,033-21,041, 1994.

Hoell, J.M., D.D. Davis, S.C. Liu, R. Newell, M. Shipham, H. Akimoto, R.J. McNeal, R.J. Bendura, and J.W. Drewry, Pacific Exploratory Mission–West A (PEM-West A): September-October 1991, *J. Geophys. Res.*, *101*, 1641-1653, 1996.

Jacob, D.J., and M.J. Prather, Radon-222 as a test of convection in a general circulation model, *Tellus*, *42*, 118-134, 1990.

Jacob, D.J., S. Sillman, J.A. Logan, and S.C. Wofsy, Least independent variables method for simulation of tropospheric ozone, *J. Geophys. Res.*, *94*, 8497-8509, 1989.

Jacob, D.J., J.A. Logan, G.M. Gardner, R.M. Yevich, C.M. Spivakovsky, S.C. Wofsy, S. Sillman, and M.J. Prather, Factors regulating ozone over the United States and its export to the global atmosphere, *J. Geophys. Res.*, *98*, 14,817-14,826, 1993a.

Jacob, D.J., et al., Simulation of summertime ozone over North America, *J. Geophys. Res.*, *98*, 14,797-14,816, 1993b.

Jacobson, M.Z., and R.P. Turco, SMVGEAR: A sparse-matrix, vectorized GEAR code for atmospheric transport models, *Atmos. Environ.*, *28*, 273-284, 1994.

Jaeglé, L., D.J. Jacob, Y. Wang, A.J. Weinheimer, B.A. Ridley, T.L. Campos, G.W. Sachse, and D. Hagen, Origin of NO_y in the upper troposphere over the central United States, *Geophys. Res. Lett.*, in press, 1997.

Kames, J., and U. Schurath, Alkyl nitrates and bifunctional nitrates of atmospheric interest: Henry's law constants and their temperature dependencies, *J. Atmos. Chem.*, *15*, 79-95, 1992.

Kasibhatla, P.S., NO_y from subsonic aircraft emissions: A global three-dimensional model study, *Geophys. Res. Lett.*, *20*, 1707-1710, 1993.

Kasibhatla, P.S., H. Levy II, and W.J. Moxim, Global NO_y, HNO_3, PAN, and NO_y distributions from fossil fuel combustion emissions: A model study, *J. Geophys. Res.*, *98*, 7165-7180, 1993.

Kirchner, F., and W.R. Stockwell, The effect of peroxy radical reactions on the predicted concentrations of ozone, nitrogenous compounds, and radicals, *J. Geophys. Res.*, *101*, 21,007-21,022, 1996.

Kleinman, L., et al., Ozone formation at a rural site in the southeastern United States, *J. Geophys. Res.*, *99*, 3469-3482, 1994.

Kleinman, L., Y.-N. Lee, S.R. Springston, J.H. Lee, L. Nunnermacker, J. Weinstein-Lloyd, X. Zhou, and L. Newman, Peroxy radical concentration and ozone formation rate at a rural site in the southeastern United States, *J. Geophys. Res.*, *100*, 7263-7273, 1995.

Lamarque, J.-F., G.P. Brasseur, P.G. Hess, and J.F. Müller, Three-dimensional study of the relative contributions of the different nitrogen sources in the troposphere, *J. Geophys. Res.*, *101*, 22,955-22,968, 1996.

Lamb, B., A. Guenther, D. Gay, and H. Westberg, A national inventory of biogenic hydrocarbon emissions, *Atmos. Environ.*, *21*, 1695-1705, 1987.

Lee, Y.-N., X. Zhou, and K. Hallock, Atmospheric carbonyl compounds at a rural southeastern United States site, *J. Geophys. Res.*, *100*, 25,933-25,944, 1995.

Liang, J., and D.J. Jacob, Effect of aqueous phase cloud chemistry on tropospheric ozone, *J. Geophys. Res.*, *102*, 5993-6001, 1997.

Liang, J., L.W. Horowitz, D.J. Jacob, Y. Wang, A.M. Fiore, J.A. Logan, G.M. Gardner, and J.W. Munger, Seasonal budgets of reactive nitrogen species and ozone over the United States, and export fluxes to the global atmosphere, *J. Geophys. Res.*, this issue.

Lightfoot, P.D., R.A. Cox, J.N. Crowley, M. Destriau, G.D. Hayman, M.E. Jenkin, G.K. Moortgat, and F. Zabel, Organic peroxy radicals: Kinetics, spectroscopy and tropospheric chemistry, *Atmos. Environ., Part A*, *26*, 1805-1961, 1992.

Liu, S.C., M. Trainer, F.C. Fehsenfeld, D.D. Parrish, E.J. Williams, D.W. Fahey, G. Hübler, and P.C. Murphy, Ozone production in the rural troposphere and the implications for regional and global ozone distributions, *J. Geophys. Res.*, *92*, 4191-4207, 1987.

Lloyd, A.C., R. Atkinson, F.W. Lurmann, and B. Nitta, Modeling potential ozone impacts from natural hydrocarbons, I, Development and testing of a chemical mechanism for the NO_x-air photooxidations of isoprene and α-pinene under ambient conditions, *Atmos. Environ.*, *17*, 1931-1950, 1983.

Logan, J.A., Trends in the vertical distribution of ozone: An analysis of ozonesonde data, *J. Geophys. Res.*, *99*, 25,553-25,585, 1994.

Logan, J.A., M.J. Prather, S.C. Wofsy, and M.B. McElroy, Tropospheric chemistry: A global perspective, *J. Geophys. Res.*, *86*, 7210-7254, 1981.

Luke, W.T., R.R. Dickerson, and L.J. Nunnermacker, Direct measurement of the photolysis rate coefficients and Henry's law constants of several alkyl nitrates, *J. Geophys. Res.*, *94*, 14,905-14,921, 1989.

Lurmann, F.W., A.C. Lloyd, and R. Atkinson, A chemical mechanism for use in long-range transport/acid deposition computer modeling, *J. Geophys. Res.*, *91*, 10,905-10,936, 1986.

Martin, R.S., H. Westberg, E. Allwine, L. Ashman, J.C. Farmer, and B. Lamb, Measurement of isoprene and its atmospheric oxidation products in a central Pennsylvania deciduous forest, *J. Atmos. Chem.*, *13*, 1-32, 1991.

Mauzerall, D.L., D.J. Jacob, S.-M. Fan, J.D. Bradshaw, G.L. Gregory, G.W. Sachse, and D.R. Blake, Origin of tropospheric ozone at remote high northern latitudes in summer, *J. Geophys. Res.*, *101*, 4175-4188, 1996.

McKeen, S.A., E.-Y. Hsie, M. Trainer, R. Tallamraju, and S.C. Liu, A regional model study of the ozone budget in the eastern United States, *J. Geophys. Res.*, *96*, 10,809-10,845, 1991a.

McKeen, S.A., E.-Y. Hsie, and S.C. Liu, A study of the dependence of rural ozone on ozone precursors in the eastern United States, *J. Geophys. Res.*, *96*, 15,377-15,394, 1991b.

McKeen, S.A., et al., Photochemical modeling of hydroxyl and its relationship to other species during the Tropospheric OH Photochemistry Experiment, *J. Geophys. Res.*, *102*, 6467-6493, 1997.

Michelson, H.A., R.J. Salawitch, P.O. Wennberg, and J.G. Anderson, Production of $O(^1D)$ from photolysis of O_3, *Geophys. Res. Lett.*, *21*, 2227-2230, 1994.

Montzka, S.A., M. Trainer, P.D. Goldan, W.C. Kuster, and F.C. Fehsenfeld, Isoprene and its oxidation products, methyl vinyl ketone and methacrolein, in the rural troposphere, *J. Geophys. Res.*, *98*, 1101-1111, 1993.

Montzka, S.A., M. Trainer, W.M. Angevine, and F.C. Fehsenfeld, Measurements of 3-methyl furan, methyl vinyl ketone, and methacrolein at a rural forested site in the southeastern United States, *J. Geophys. Res.*, *100*, 11,393-11,401, 1995.

Moxim, W.J., H. Levy II, and P.S. Kasibhatla, Simulated global tropospheric PAN: Its transport and impact on NO_x, *J. Geophys. Res.*, *101*, 12,621-12,638, 1996.

Mozurkewich, M., P.H. McMurry, A. Gupta, and J.G. Calvert, Mass accommodation coefficient for HO_2 radicals on aqueous particles, *J. Geophys. Res.*, *92*, 4163-4170, 1987.

Munger, J.W., D.J. Jacob, B.C. Daube, L.W. Horowitz, W.C. Keene, and B.G. Heikes, Formaldehyde, glyoxal, and methylglyoxal in air and cloudwater at a rural mountain site in central Virginia, *J. Geophys. Res.*, *100*, 9325-9333, 1995.

Munger, J.W., S.C. Wofsy, P.S. Bakwin, S.-M. Fan, M.L. Goulden, B.C Daube, A.H. Goldstein, K.E. Moore, and D.R. Fitzjarrald, Atmospheric deposition of reactive nitrogen oxides and ozone in a temperate deciduous forest and a subarctic woodland, 1, Measurements and mechanisms, *J. Geophys. Res.*, *101*, 12,639-12,657, 1996.

Muthuramu, K., P.B. Shepson, and J.M. O'Brien, Preparation, analysis, and atmospheric production of multifunctional organic nitrates, *Environ. Sci. Technol.*, *27*, 1117-1124, 1993.

National Research Council (NRC), *Rethinking the Ozone Problem in Urban and Regional Air Pollution*, Nat. Acad. Press, Washington, D.C., 1991.

Olszyna, K.J., E.M. Bailey, R. Simonaitis, and J.F. Meagher, O_3 and NO_y relationships at a rural site, *J. Geophys. Res.*, *99*, 14,557-14,563, 1994.

O'Sullivan, D.W., M. Lee, B.C. Noone, and B.G. Heikes, Henry's law constant determinations for hydrogen peroxide, methyl hydroperoxide, hydroxymethyl hydroperoxide, ethyl hydroperoxide, and peroxyacetic acid, *J. Phys. Chem.*, *100*, 3241-3247, 1996.

Parrish, D.D., et al., Systematic variations in the concentration of NO_y (NO plus NO_2) at Niwot Ridge, Colorado, *J. Geophys. Res.*, *95*, 1817-1836, 1990.

Parrish, D.D., M. Trainer, M.P. Buhr, B.A. Watkins, and F.C. Fehsenfeld, Carbon monoxide concentrations and their relation to concentrations of total reactive oxidized nitrogen at two rural U.S. sites, *J. Geophys. Res.*, *96*, 9309-9320, 1991.

Parrish, D.D., J.S. Holloway, M. Trainer, P.C. Murphy, G.L. Forbes, and F.C. Fehsenfeld, Export of North American ozone pollution to the North Atlantic Ocean, *Science*, *259*, 1436-1439, 1993a.

Parrish, D.D., et al., The total reactive oxidized nitrogen levels and the partitioning between the individual species at six rural sites in eastern North America, *J. Geophys. Res.*, *98*, 2927-2939, 1993b.

Paulson, S.E., and J.H. Seinfeld, Development and evaluation of a photooxidation mechanism for isoprene, *J. Geophys. Res.*, *97*, 20,703-20,715, 1992.

Paulson, S.E., R.C. Flagan, and J.H. Seinfeld, Atmospheric photooxidation of isoprene, II, The ozone-isoprene reaction, *Int. J. Chem. Kinet.*, *24*, 103-125, 1992.

Piccot, S.D., J.J. Watson, and J.W. Jones, A global inventory of volatile organic compound emissions from anthropogenic sources, *J. Geophys. Res.*, *97*, 9897-9912, 1992.

Plummer, D.A., J.C. McConnell, P.B. Shepson, D.R. Hastie, and H. Niki, Modeling of ozone formation at a rural site in southern Ontario, *Atmos. Environ.*, *30*, 2195-2217, 1996.

Poulida, O., R.R. Dickerson, B.G. Doddridge, J.Z. Holland, R.G. Wardell, and J.G. Watkins, Trace gas concentrations and meteorology in rural Virginia, 1, Ozone and carbon monoxide, *J. Geophys. Res.*, *96*, 22,461-22,475, 1991.

Poulida, O., K.L. Civerolo, and R.R. Dickerson, Observations and tropospheric photochemistry in central North Carolina, *J. Geophys. Res.*, *99*, 10,553-10,563, 1994.

Prather, M.J., Numerical advection by conservation of second-order moments, *J. Geophys. Res.*, *91*, 6671-6681, 1986.

Prather, M.J., M.C. McElroy, S. Wofsy, G. Russell, and D. Rind, Chemistry of the global troposphere: Fluorocarbons as tracers of air motions, *J. Geophys. Res.*, *92*, 6579-6613, 1987.

Raber, W.H., and G.K. Moortgat, Photooxidation of selected carbonyl compounds in air: Methyl ethyl ketone, methyl vinyl ketone, methacrolein and methyl glyoxal, in *Problems and Progress in Atmospheric Chemistry, Advances in Physical Chemistry*, edited by J.R. Barker, World Sci., River Edge, N. J., 1995.

Roberts, J.M., The atmospheric chemistry of organic nitrates, *Atmos. Environ., Part A*, *24*, 243-287, 1990.

Roberts, J.M., and R.W. Fajer, UV absorption cross sections of organic nitrates of potential atmospheric importance and estimation of atmospheric lifetimes, *Environ. Sci. Technol.*, *23*, 945-951, 1989.

Roberts, J.M., et al., Relationships between PAN and ozone at sites in eastern North America, *J. Geophys. Res.*, *100*, 22,821-22,830, 1995.

Ross, H.B., and K.J. Noone, A numerical investigation of the destruction of peroxy radical by Cu ion catalyzed reactions on atmospheric particles, *J. Atmos. Chem.*, *12*, 121-136, 1991.

Rowley, D.M., R. Lesclaux, P.D. Lightfoot, K. Hughes, M.D. Hurley, S. Rudy, and T.J. Wallington, A kinetic and mechanistic study of the reaction of neopentyl peroxy radicals with HO_2, *J. Phys. Chem.*, *96*, 7043-7048, 1992.

Schwartz, S.E., Gas- and aqueous-phase chemistry of HO_2 in liquid water clouds, *J. Geophys. Res.*, *89*, 11,589-11,598, 1984.

Shepson, P.B., D.R. Hastie, H.I. Schiff, M. Polizzi, J.W. Bottenheim, K. Anlauf, G.I. Mackay, and D.R. Karecki, Atmospheric concentrations and temporal variations of C_1-C_3 carbonyl compounds at two rural sites in central Ontario, *Atmos. Environ., Part A*, *25*, 2001-2015, 1991.

Shepson, P.B., E. Mackay, and K. Muthuramu, Henry's law constants and removal processes for several atmospheric β-hydroxy alkyl nitrates, *Environ. Sci. Technol.*, *30*, 3618-3623, 1996.

Sillman, S., J.A. Logan, and S.C. Wofsy, The sensitivity of ozone to nitrogen oxides and hydrocarbons in regional ozone episodes, *J. Geophys. Res.*, *95*, 1837-1851, 1990.

Singh, H.B., D. O'Hara, D. Herlth, W. Sachse, D.R. Blake, J.D. Bradshaw, M. Kanakidou, and P.J. Crutzen, Acetone in the atmosphere: Distribution, sources, and sinks, *J. Geophys. Res.*, *99*, 1805-1819, 1994a.

Singh, H.B., et al., Summertime distribution of PAN and other reactive nitrogen species in the northern high-latitude atmosphere of eastern Canada, *J. Geophys. Res.*, *99*, 1821-1835, 1994b.

Spivakovsky, C.M., R. Yevich, J.A. Logan, S.C. Wofsy, M.B. McElroy, and M.J. Prather, Troposhperic OH in a three-dimensional chemical tracer model: An assessment based on observations of CH_3CCl_3, *J. Geophys. Res.*, *95*, 18,441-18,471, 1990.

Stevens, P.S., et al., HO_2/OH and RO_2/HO_2 ratios during the Tropospheric OH Photochemistry Experiment: Measurement and theory, *J. Geophys. Res.*, *102*, 6379-6391, 1997.

Stockwell, W.R., P. Middleton, J.S. Chang, and X. Tang, The second generation regional acid deposition model chemical mechanism for regional air quality modeling, *J. Geophys. Res.*, *95*, 16,343-16,367, 1990.

Stockwell, W.R., J.B. Milford, D. Gao, and Y.-J. Yang, The effect of acetyl peroxy-peroxy radical reactions on peroxyacetyl nitrate and ozone concentrations, *Atmos. Environ.*, *29*, 1591-1599, 1995.

Talukdar, R.K., J.B. Burkholder, A.-M. Schmoltner, J.M. Roberts, R.R. Wilson, and A.R. Ravishankara, Investigation of the loss processes for peroxyacetyl nitrate in the atmosphere: UV photolysis and reaction with OH, *J. Geophys. Res.*, *100*, 14,163-14,173, 1995.

Thompson, A.M., The oxidizing capacity of Earth's atmopshere: Probable past and future changes, *Science*, *256*, 1157-1165, 1992.

Trainer, M., E.J. Williams, D.D. Parrish, M.P. Buhr, E.J. Allwine, H.H. Westberg, F.C. Fehsenfeld, and S.C. Liu, Models and observations of the impact of natural hydrocarbons on rural ozone, *Nature*, *329*, 705-707, 1987.

Trainer, M., et al., Observations and modeling of the reactive nitrogen photochemistry at a rural site, *J. Geophys. Res.*, *96*, 3045-3063, 1991.

Trainer, M., et al., Correlation of ozone with NO_y in photochemically aged air, *J. Geophys. Res.*, *98*, 2917-2925, 1993.

Tuazon, E.C., and R. Atkinson, A product study of the gas-phase reaction of methyl vinyl ketone with the OH radical in the presence of NO_x, *Int. J. Chem. Kinet.*, *21*, 1141-1152, 1989.

Tuazon, E.C., and R. Atkinson, A product study of the gas-phase reaction of isoprene with the OH radical in the presence of NO_x, *Int. J. Chem. Kinet.*, *22*, 1221-1236, 1990a.

Tuazon, E.C., and R. Atkinson, A product study of the gas-phase reaction of methacrolein with the OH radical in the presence of NO_x, *Int. J. Chem. Kinet.*, *22*, 591-602, 1990b.

Wang, Y., D.J. Jacob, J.A. Logan, and C.M. Spivakovsky, Global simulation of tropospheric O_3-NO_x-hydrocarbon chemistry, 1, Model formulation, *J. Geophys. Res.*, in press, 1997a.

Wang, Y., J.A. Logan, D.J. Jacob, and C.M. Spivakovsky, Global simulation of tropospheric O_3-NO_x-hydrocarbon chemistry, 2, Model evaluation and global ozone budget, *J. Geophys. Res.*, in press, 1997b.

Wang, Y., D.J. Jacob, and J.A. Logan, Global simulation of tropospheric O_3-NO_x-hydrocarbon chemistry, 3, Origin of tropospheric ozone and effects of non-methane hydrocarbons, *J. Geophys. Res.*, in press, 1997c.

Watkins, B.A., D.D. Parrish, M. Trainer, R.B. Norton, J.E. Yee, F.C. Fehsenfeld, and B.G Heikes, Factors influencing the concentration of gas phase hydrogen peroxide during the summer at Niwot Ridge, Colorado, *J. Geophys. Res.*, *100*, 22,831-22,840, 1995a.

Watkins, B.A., D.D. Parrish, S. Buhr, R.B. Norton, M. Trainer, J.E. Yee, and F.C. Fehsenfeld, Factors influencing the concentration of gas phase hydrogen peroxide during the summer at Kinterbish, Alabama, *J. Geophys. Res.*, *100*, 22,841-22,851, 1995b.

Wesely, M.L., Parameterization of surface resistance to gaseous dry deposition in regional-scale numerical models, *Atmos. Environ.*, *23*, 1293-1304, 1989.

Zhou, X., and Y.-N. Lee, Aqueous solubility and reaction kinetics of hydroxymethyl hydroperoxide, *J. Phys. Chem.*, *96*, 265-272, 1992.

G. M. Gardner and D. J. Jacob, Division of Engineering and Applied Sciences and Department of Earth and Planetary Sciences, Harvard University, Cambridge, MA 02138. (email: gmg@io.harvard.edu; djj@io.harvard.edu)

L. W. Horowitz (corresponding author), NCAR/ASP, P.O. Box 3000, Boulder, CO 80307-3000. (email: lwh@io.harvard.edu)

J. Liang, Department of Civil and Environmental Engineering, Stanford University, Sanford, CA 94041. (email: jyl@neap.stanford.edu)

(Received May 5, 1997; revised October 17, 1997;
accepted October 28, 1997.)